Utilizing Artificial Intelligence (AI) for the optimal design of geothermal cogeneration systems in zero energy building

Results in Engineering 26 (2025) 104873

Contents lists available at ScienceDirect

Results in Engineering

journal homepage: www.sciencedirect.com/journal/results-in-engineering

Research paper

Utilizing Artificial Intelligence (AI) for the optimal design of geothermal cogeneration systems in zero energy building

Ehsanolah Assareh [a], Mohammad Zoghi [b], Ali Zare [b], Hassan Bazazzadeh [c,*], Adnan Alboghobeysh [d], Saleh Mobayen [e], Nima Izadyar [a,f], Siamak Hoseinzadeh [g]

[a] Built Environment and Engineering Program, College of Sport, Health and Engineering (CoSHE), Victoria University, Melbourne, VIC 3011, Australia
[b] School of Engineering, Deakin University, Geelong, VIC 3216, Australia
[c] Urban Energy Systems Lab, Swiss Federal Laboratories of Material Science and Technology (Empa), Ueberlandstrasse 129, 8600, Dübendorf, Switzerland
[d] Department of Mechanical Engineering, Arvandan Non-profit Higher Education Institute, Khorramshahr, Iran
[e] Graduate School of Intelligent Data Science, National Yunlin University of Science and Technology, Douliou, Yunlin 640301, Taiwan
[f] Institute for Sustainable Industries and Liveable Cities, Victoria University, Melbourne, VIC 3011, Australia
[g] Department of Planning, Design, and Technology of Architecture Sapienza University of Rome, Rome 00196, Italy

A R T I C L E I N F O

Keywords:
Modified organic rankine cycle
Artificial intelligence (AI)
Geothermal energy
Residential building
Multi Energy Production System
BEopt
Zero Energy Building (ZEB)

A B S T R A C T

This research investigates the design and optimization of energy consumption for a five-story residential building in Copenhagen, Denmark, comprising ten units of 100 square meters each. The primary objective is to achieve the Zero Energy Building (ZEB) standard. Utilizing BEopt software for simulation and optimization, the study found that the building's annual electricity consumption is approximately 2789,416 kWh.A crucial aspect of energy analysis is the building's orientation. As energy optimization becomes increasingly vital, this research not only focuses on enhancing the building's energy system but also evaluates the optimal directional placement of the structure. The analysis revealed that the south-facing orientation results in the lowest cooling energy consumption at 90,511 kWh, while the east side records the least heating energy consumption at approximately 2133,357 kWh.To fulfill the building's energy requirements, a renewable geothermal energy system was proposed, capable of generating electricity, cooling, and heating. This proposed co-generation system incorporates a modified Organic Rankine Cycle (ORC) equipped with an ejector and preheater for electricity generation, utilizing waste heat for cooling and heating purposes. Modeling was conducted using the widely recognized EES software, while system optimization employed a combination of neural networks and intelligent optimization algorithms. The optimized configuration achieved an exergy efficiency of 63.79 % and a cost rate of $57.82 per hour. Economic analysis indicated that the heat recovery steam generator (HRVG) incurs the highest cost rate at $20.06 per hour. Additionally, a feasibility study incorporating Copenhagen's climate data demonstrated that the system could produce 10,465,920 kWh of electricity, 6340,320 kWh of cooling, and 7160,992 kWh of heating annually. The findings confirm that the geothermal system can adequately meet the energy demands of the five-story residential building throughout in one year.

1. Introduction

Growing global concerns over the depletion of fossil fuels and the escalating environmental pollution have led to an increased focus on renewable energy sources [1]. Renewable energy refers to the types of energy that can be replenished naturally. Geothermal energy is one of the most promising of these energy sources. The potential of geothermal energy resources to meet the world's energy demand is remarkably high [2]. Geothermal energy is the thermal energy that is naturally stored within the solid outer layer of the Earth, known as the crust. This energy originates from two primary sources: the residual heat from the planet's formation and the continuous decay of radioactive elements that are present deep within the Earth's interior, particularly in the molten mantle and core regions. In essence, geothermal energy represents the natural heat that is continuously generated and retained within the Earth's subsurface layers, which can be extracted and utilized to meet various human energy requirements. The Earth's interior is composed of several concentric layers, each with distinct physical and chemical properties. The innermost layer is the core, which is primarily composed

* Corresponding author.
E-mail address: Hassan.bazazzadeh@empa.ch (H. Bazazzadeh).

https://doi.org/10.1016/j.rineng.2025.104873
Received 2 December 2024; Received in revised form 17 February 2025; Accepted 9 April 2025
Available online 18 April 2025

Nomenclature

T_0	Ambient temperature [°C]
P_0	Ambient pressure [kPa]
C_P	Specific heat of air and water at constant pressure [kJ/kg.K]
$\dot{E}x$	Exergy [kW]
s	Specific entropy [kJ/kg.K]
$\dot{m}$	Mass flow rate [kg/s]
T	Temperature [°C]
h	Specific enthalpy [kj/kg]
x	Salinity [ppm]
Z	Investment cost [$]
$\dot{Z}$	Cost rate [$/h]
$\dot{Q}$	Heat transfer rate [kW]
W	Power [kW]
m	mass

Subscripts

ch	Chemical
pH	physical
cv	control volume
pp	pinch point
k	The interest rate
ex	exergy
n	Period of performance
T	Interest rate and performance period
0	Initial mode
i	Secondary mode

Abbreviations

HRVG	Heat recovery vapour generator
CRF	Capital Recover Factor
tur	Turbine
cond	Condenser
eva	Evaporator
HEX	Heat exchanger
PreH	Preheater
ORC	Organic Rankine Cycle
GEO	Geothermal energy

Greek symbol

η	efficiency
φ	Maintenance factor

of iron and nickel and exists in both solid and liquid states. Surrounding the core is the mantle, a thick layer of molten and semi-molten rock that accounts for the majority of the Earth's volume. The outermost layer is the crust, which is relatively thin compared to the other layers and is composed of various types of solid rock. It is within the crust that geothermal energy is primarily concentrated and can be accessed for practical applications [3]. The application of geothermal energy in sustainable energy production systems has garnered significant attention in recent years. By harnessing the thermal energy and temperature gradients found in the earth's subsurface, geothermal energy-based technologies produce clean electrical energy [4]. In this research, the thermal energy from the earth has been harnessed to supply the energy needs of a building, including heating, cooling, and electricity. The integration of geothermal energy into building design has gained significant traction in recent years, as it presents a sustainable and efficient solution for energy consumption. Innovative approaches are being implemented in this field, making it a compelling area of study. This research employs an artificial intelligence-optimized system that utilizes geothermal heat to meet the building's energy requirements. This approach is particularly appealing due to its synergy with an optimally designed building that considers various performance parameters. By leveraging advanced AI techniques, the system can dynamically adjust to changing energy demands and environmental conditions, enhancing overall efficiency. Additionally, the research emphasizes the importance of selecting the optimal orientation for the building. Through careful analysis, the study identifies how the building's direction can significantly impact energy efficiency and consumption. This focus on orientation, combined with the use of geothermal energy, results in a highly attractive and practical solution for achieving a zero-energy building. By incorporating innovative concepts and state-of-the-art technologies, this research contributes to the development of zero energy buildings, showcasing the potential of geothermal energy as a reliable and sustainable energy source. The findings underscore the viability of integrating geothermal systems into modern architecture, paving the way for more environmentally friendly and energy-efficient building practices. Zero energy buildings are designed to achieve net-zero annual energy consumption and net-zero carbon emissions. These buildings are capable of operating independently from the main energy supply grid, making them self-sufficient in terms of energy consumption and production [5]. In a zero-energy building, energy is generated locally through a combination of renewable energy technologies. This approach allows for the efficient utilization of available renewable resources within the building's vicinity, minimizing the need for external energy sources and reducing the environmental impact associated with energy generation. One of the key advantages of zero energy buildings is their ability to meet all energy requirements in a cost-effective manner. By harnessing local renewable sources and employing advanced energy-efficient technologies, these buildings can achieve energy independence while maintaining affordability for occupants. A crucial characteristic of zero energy buildings is the absence of conventional fuel usage. Instead, these buildings rely entirely on renewable energy sources to power their operations [6]. The annual energy consumption of a zero-energy building is balanced by its annual renewable energy production, ensuring a net-zero energy balance over the course of a year. By eliminating fossil fuel use and achieving net-zero energy consumption, zero energy buildings greatly aid in lowering greenhouse gas emissions and minimizing the effects of climate change. These buildings serve as models for sustainable development, demonstrating the feasibility and benefits of integrating renewable energy technologies into the built environment [7].

Despite the promising potential of geothermal energy systems, the research background in this specific field is limited due to the novelty of the proposed system and the scarcity of studies focusing solely on geothermal energy. The lack of extensive research in this area presents both challenges and opportunities for further exploration and innovation. One of the main challenges in this field is the limited availability of empirical data and case studies to validate the performance and feasibility of geothermal-based systems. Without a robust body of research, decision-makers and stakeholders may be hesitant to invest in and adopt these technologies, hindering their widespread implementation.

However, the novelty of the proposed system also presents a unique opportunity for researchers to contribute to the advancement of geothermal energy applications. By conducting comprehensive studies, developing innovative system designs, and demonstrating the viability of geothermal energy in various contexts, researchers can fill the existing knowledge gaps and pave the way for the widespread adoption of these technologies. Moreover, the limited research background in this field underscores the importance of interdisciplinary collaboration among experts from fields such as energy engineering, materials science, and environmental science. By combining their expertise and perspectives, researchers can develop holistic solutions that address the technical, economic, and environmental aspects of geothermal energy systems. As the global demand for renewable and sustainable energy solutions continues to grow, the need for robust research in the field of geothermal energy systems becomes increasingly pressing. By addressing the research gaps and exploring the untapped potential of geothermal energy, researchers can contribute to the development of a more sustainable and resilient energy future. In this section, we will review several studies that align with the current research to highlight its significance and contextualize its contributions to the field. By examining relevant literature, we aim to underscore the importance of integrating geothermal energy systems into building design, particularly in the pursuit of zero energy buildings.

Mohammadi et al. (2024) evaluated battery and hydrogen energy storage systems for near-zero energy buildings. A building in Bandar Abbas, Iran was considered in this study. The main objective of this case study is to compare two different energy storage methods. The results show that battery and H2 storage systems generate 39 and 37 % of the electricity required by the buildings, respectively [8].

Shirazi et al. (2024) investigated efficient thermal energy storage for decarbonizing residential buildings in cold climates. The system has an energy cost of $78.9 per MWh (heating and electricity) which is attributed to the developed controllers applied to thermal energy storage [9].

Mohammadi et al. (2023) evaluated a geothermal and solar hybrid system. The outputs of the system were heating, cooling, electricity, and fresh water. The results show that the proposed system can achieve 25.4 % exergy efficiency and 34.1 $/GJ total unit cost of products, which shows 48 % and 43 % improvement compared to the baseline case study [10].

Sohani et al. (2023) designed a renewable energy-based multi-generation system for electricity, heating, cooling, hydrogen, and water with phase change materials. The results showed that by applying multi-objective optimization, electricity, heating, cooling, hydrogen, and water production are achieved by 16.4, 12.7, 8.4, 10.3, and 9.5 % compared to the system without PCM [11].

Alibaba et al. examined an ORC-equipped hybrid power station that integrated solar and geothermal energy in 2020. The concentrated solar energy was supplemented by the geothermal power plant. For the purpose of producing building heating and cooling power, a seperate geothermal cycle (first mode) and a hybrid geothermal-solar system (second mode) were studied. The findings showed that the combined system of two renewable energies performed better [12].

Kavian et al. optimized a solar/geothermal co-generation system in 2020 to fulfill the year-round heating and cooling bar requirements of a zero-energy building (ZEB) by analyzing energy system, financial, and environmental aspects. The findings demonstrated that, among many schemes, a 35 m2 solar panel with a 31 % solar portion can be economically viable up to a 24 % inflation rate [13].

Guler et al. assessed the effectiveness of a geothermal and solar-powered multigeneration system in 2022. Three separate models were created for this purpose. These models were verified for a real-world area in Turkey using actual solar and geothermal data. The passing stream is 85 kg/s and the temperature of the geothermal source is 130 0C. Homes are heated with the systems' leftover heat [14].

In 2022, Shumiye et al. investigated the exergy of the geothermal-solar power plant. The objectives are cost-effectiveness, reduced waste heat, enhanced exergetic efficiency (η_{ex}), and advanced power generation, boiling, and water treatment. The system's target of 44 MWh of power with an average η_{ex} of 50.4 % was met [15].

In 2020, Haideranjad et al. worked on the optimization of a geothermal power generation unit using biomass to produce clean electricity.The system's energy efficiency (η_{en}) and η_{ex} can reach 13.9 % and 19.4 %, respectively, according to the results, and its overall cost rate was predicted to be 285.3 $/h [16].

In 2019, Kahraman and colleagues analyzed a 21 MW geothermal power plant using air conditioning. The ORC was investigated numerically based on operational data and design data. The effect of ambient temperature on total production costs, energy efficiency, and exergy was investigated in this research. The results indicated an increase in the efficiency of the power plant [17].

A novel geothermal-solar-wind energy production system was the subject of multi-objective analysis and optimization in 2023 by Bamisile et al. The system's overall η_{en} and η_{ex} was found to be 48.61 % and 88.31 %, respectively. If the system is optimized based on η_{ex}, these efficiency levels can be raised to 51.76 % and 95.08 % [18].

Zhang et al. examined the thermodynamic performance of a modified coal-fired power plant in 2022 and examined how it coupled geothermal energy with ORC to boost power output capacity. The findings demonstrated that by using some medium-temperature steam from ST to power the ORC with discharged steam as a preheating heat source, the thermodynamic performance of the entire system may be enhanced [19].

Tekkanat et al. assessed the production of hydrogen using a multi-generation system based on geothermal energy in 2023. The system's overall production power is 1951 kW, the rate at which hydrogen is produced is 0.0015 kg/s, and the overall η_{en} and η_{ex} is 59.53 % and 53.17 %, according to the results. The multigeneration system's economic study revealed that the levelized energy cost is 0.102 $/kWh & overall cost rate ($\dot{C}_{tot}$) is 186 $/h [20].

Haris et al. studied a regenerative proposed geothermal co-generation system intended for energy storage and the production of both heat and power in 2022. According to their results, during a 30-year period, the electric potential obtained from the reservoir's temperature drops from 7.17 MW to 5.08 MW with crucial optimization of thermal production. This reduction highlights the economic feasibility of significant advancements in geothermal energy systems. Furthermore, the study revealed that the geothermal system demonstrates regenerative capabilities, as the temperature of the geological formation increases with each cycle of energy storage and recovery. These characteristic underscores the long-term sustainability and efficiency of utilizing geothermal resources for energy production [21].

The technical analysis of a novel solar-geothermal gas-based multi-generation system for the production of hot water and electricity was covered by Khoshgoftar Manesh et al. in 2022. This system produced power, hydrogen, hot water, and freshwater by means of an ORC, an internal combustion engine, a polymer electrolyte membrane, and a dehumidification desalination unit. According to the findings, the system's η_{en}, η_{ex}, total yearly cost, and environmental consequences are 23.87 %, 28.21 %, 0.144 $/kWh, and 0.024 Pts/kWh [22].

In 2023, Baniasadi et al. investigated a multi-energy generation solar-geothermal system. The purpose of this study was to evaluate the feasibility of using a solar-geothermal system for Meeting the energy and water needs of a residential building using exergy-economic indicators. The results showed that the energy efficiency of the system, as well as the exergy of the system in the cooling mode, is 13.27 and 32.44 %, and in the heating, mode is 17.25 % and 42.4 % respectively [23].

Sharmin et al. in 2023 reviewed strategies for extracting, utilizing, and improving geothermal energy. This study reviewed the relevant issues in terms of energy growth, evaluated the technologies implemented in power plants, and direct heating applications, and described the advantages and disadvantages of geothermal technology as well as the areas for growth. In addition, to improve the performance of existing conventional systems, the implementation of advanced geothermal systems and hybrid geothermal systems were proposed as suitable alternatives in this review [24].

Cao et al. in 2022 studied a geothermal-solar grid-connected energy system. The components of this system were solar panels, thermal energy storage tanks, a turbine, an absorption chiller, and a heat pump. The results showed that in addition to meeting its annual electrical demand, the system could also generate a large amount of power that

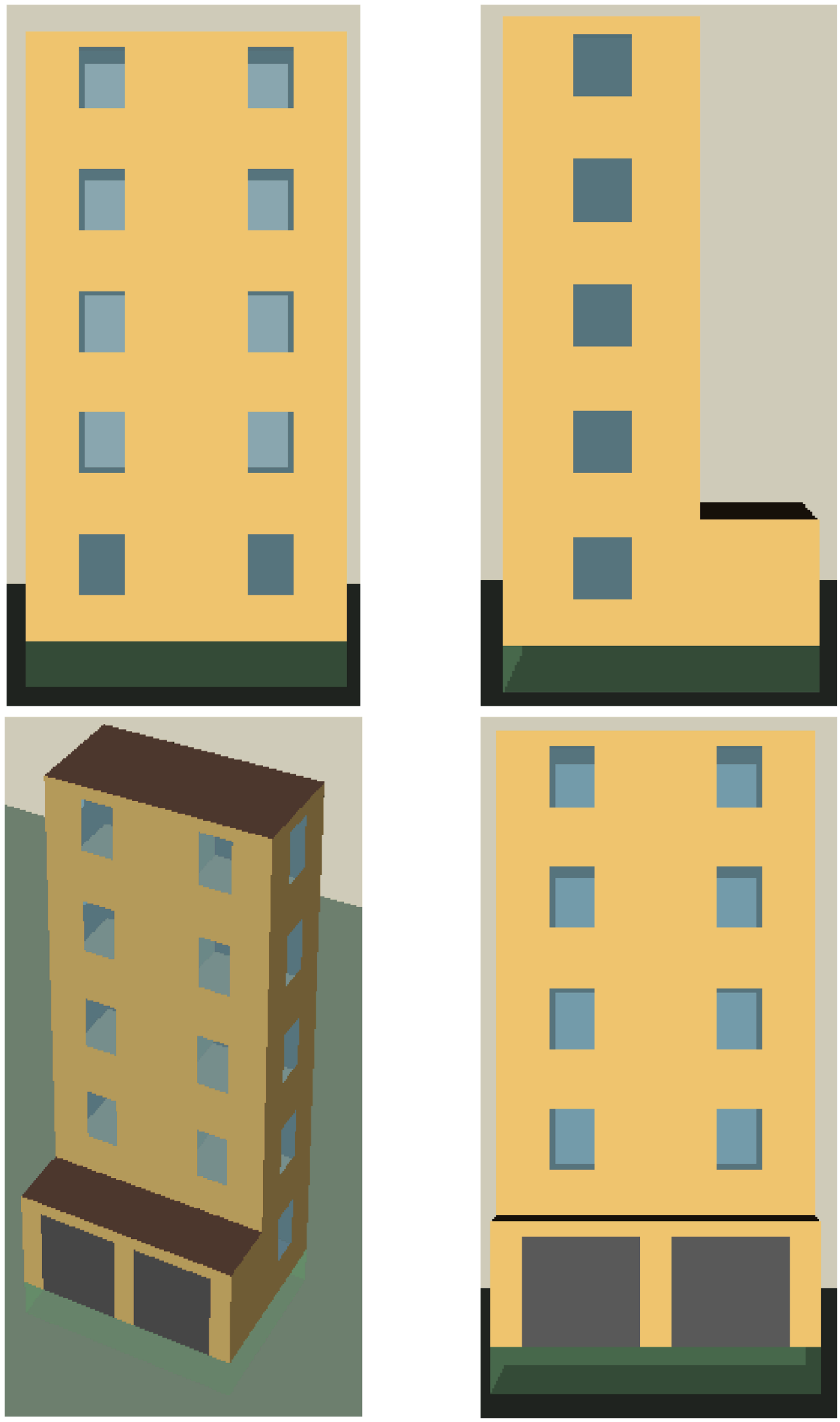

Fig. 1. View of the building.

could be sold to the national grid to offset the system costs [25].

In this section, we aim to explore the various dimensions, innovative aspects, and significance of the current research. By delving into these elements, we can better understand how this work contributes to the broader field of sustainable energy solutions and the design of residential buildings. The energy supply for residential buildings is a critical area of focus for researchers, particularly in the context of developing multi-energy production systems that incorporate geothermal energy. These systems, especially when designed with new and efficient technologies, present viable options for sustainable energy solutions. In this study, we simulate a residential building in Copenhagen, Denmark, comprising five floors with two units per floor, each unit covering an area of 100 m^2, resulting in a total building area of 1000 m^2, along with a 120 m^2 garage. We find the best energy systems for this residential complex's operation and optimize its energy consumption using the BEopt program.

The research involves a comprehensive analysis of the building's energy requirements, including the calculation of the necessary load for the entire residential complex. To ensure a thorough evaluation, we model the heating and cooling energy demands from four different orientations—north, south, east, and west. This directional analysis allows us to compare the energy consumption patterns associated with each orientation, providing valuable insights into how building placement can influence overall energy efficiency. By examining these factors, the study aims to contribute to the understanding of how multi-energy systems, particularly those utilizing geothermal energy, can be effectively integrated into residential buildings. This research not only highlights the potential for reducing energy consumption and carbon emissions but also emphasizes the importance of innovative design and technology in achieving sustainable living environments. Ultimately, the findings of this study will inform future developments in residential energy systems, supporting the transition towards more energy-efficient and environmentally friendly building practices in urban settings like Copenhagen and other cities around the globe.

The summary of this research activity can be stated as follows:

- Simulation of a 10-unit residential building using BEopt software and calculation of the building's energy consumption
- Optimization of the residential building to save energy consumption and reduce pollution emissions (selecting appropriate materials for building construction).
- Calculation of the electrical load and heating and cooling requirements of the residential building in 4 directions: north, south, east, and west.
- Use of a renewable geothermal multiple-generation system consisting of a modified organic cycle to supply the required load of the residential building.
- Optimization of the performance of the proposed renewable system to increase the exergy efficiency by reducing the cost rate of the studied geothermal system.
- Use of the neural network method as a new method for system optimization.
- Examination of the environmental performance of the proposed system.
- Calculation of the amount of energy stored during the year that is over the residential building's energy consumption produced by the system.

2. Optimal design of a residential building in copenhagen, denmark

In this study, a 5-story, 10-unit residential building in Copenhagen, Denmark is simulated to calculate its cooling, heating, and electricity consumption using BEopt software. The residential building, as shown in Fig. 1, has a total floor area of 1000 m^2, with each floor comprising two units of 100 m^2 each. Additionally, the building includes a 120 m^2 garage. BEopt (Building Energy Optimization) is a software tool used to evaluate the energy performance of residential buildings and provide cost-effective efficiency improvement solutions. For this study, the building was modeled with the following specifications:

- 5 floors, each with 2 units of 100 m^2 each
- Total building area of 1000 m^2
- 120 m^2 garage
- 2 bedrooms per residential unit
- 4 occupants per unit
- Pier foundation type

The simulation using BEopt software allowed for the estimation of the building's cooling, heating, and electricity consumption, providing valuable insights into its energy performance. By optimizing the design and incorporating energy-efficient measures, the aim is to minimize the building's energy demands and align with the principles of sustainable residential development in Copenhagen.

The necessary information in the field of collecting weather conditions in Copenhagen, including solar radiation intensity, ambient temperature, wind speed, relative humidity, and dew point, has been collected by the BEopt software database. One of the positive features of the BEopt software is its strong database.

The goal of designing with the BEopt software is to achieve an optimal level of energy saving, cost reduction, and pollution emission reduction. For this reason, during the design and simulation of the building in the BEopt software and by selecting the materials available in the BEopt database (library) according to the software framework, three goals of saving and reducing costs and reducing pollution emissions are pursued.

The BEopt software is a tool for energy optimization in buildings that is used to evaluate buildings and provide solutions to improve efficiency at the lowest cost, reduce energy consumption, and reduce pollutant emissions. In BEopt, simulation is performed based on: dimensions, architecture, building materials, number of residents, location, and facilities.

The sequential search optimization technique used by BEopt:

- Finds construction designs with minimum cost at different levels of energy savings.
- Designs the building to select appropriate materials and reduce energy consumption to reduce pollution emissions
- Identifies several nearly optimal designs along the way and enables equivalent solutions based on the preference of the builder or contractor.
- During optimization, information about the materials considered for building construction, such as costs and physical and thermal properties of the materials is effective in the optimization process, due to which the relationship between the three objectives of consumption, cost, and pollution with the properties of the materials is obtained.

Fig. 2 shows the flowchart of building analysis.

In this research, the impact of various weather parameters on the energy consumption of the residential building in Copenhagen is analyzed. The key weather factors considered include solar radiation, wind speed, ambient temperature, snowfall, and relative humidity. Fig. 3 illustrates the hourly fluctuations in these parameters throughout the year. The intensity of solar radiation in Copenhagen ranges from 0 to 900 W/h, as depicted in Fig. 3. Due to the low ambient temperatures and the significant solar radiation levels, the building's heating energy consumption remains high throughout the year. Relative humidity is typically expressed as a percentage. Fig. 3 presents the hourly changes in relative humidity for Copenhagen over the course of a year. The air temperature and humidity inside the building have a significant influence on occupant health, comfort, and well-being. Fig. 3 also shows the hourly variations in ambient temperature for Copenhagen. The results

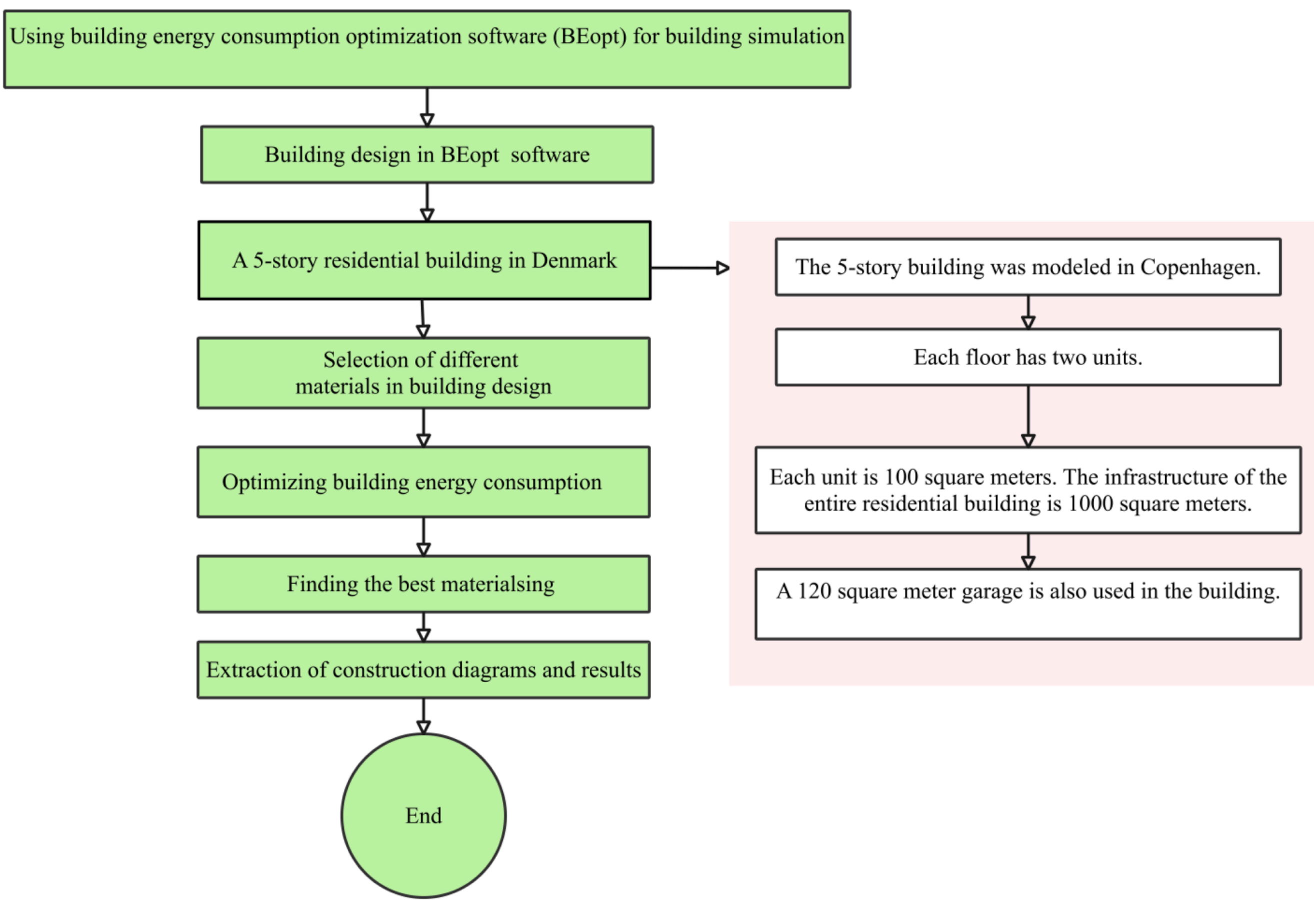

Fig. 2. Building analysis [flowchart].

unique climate.

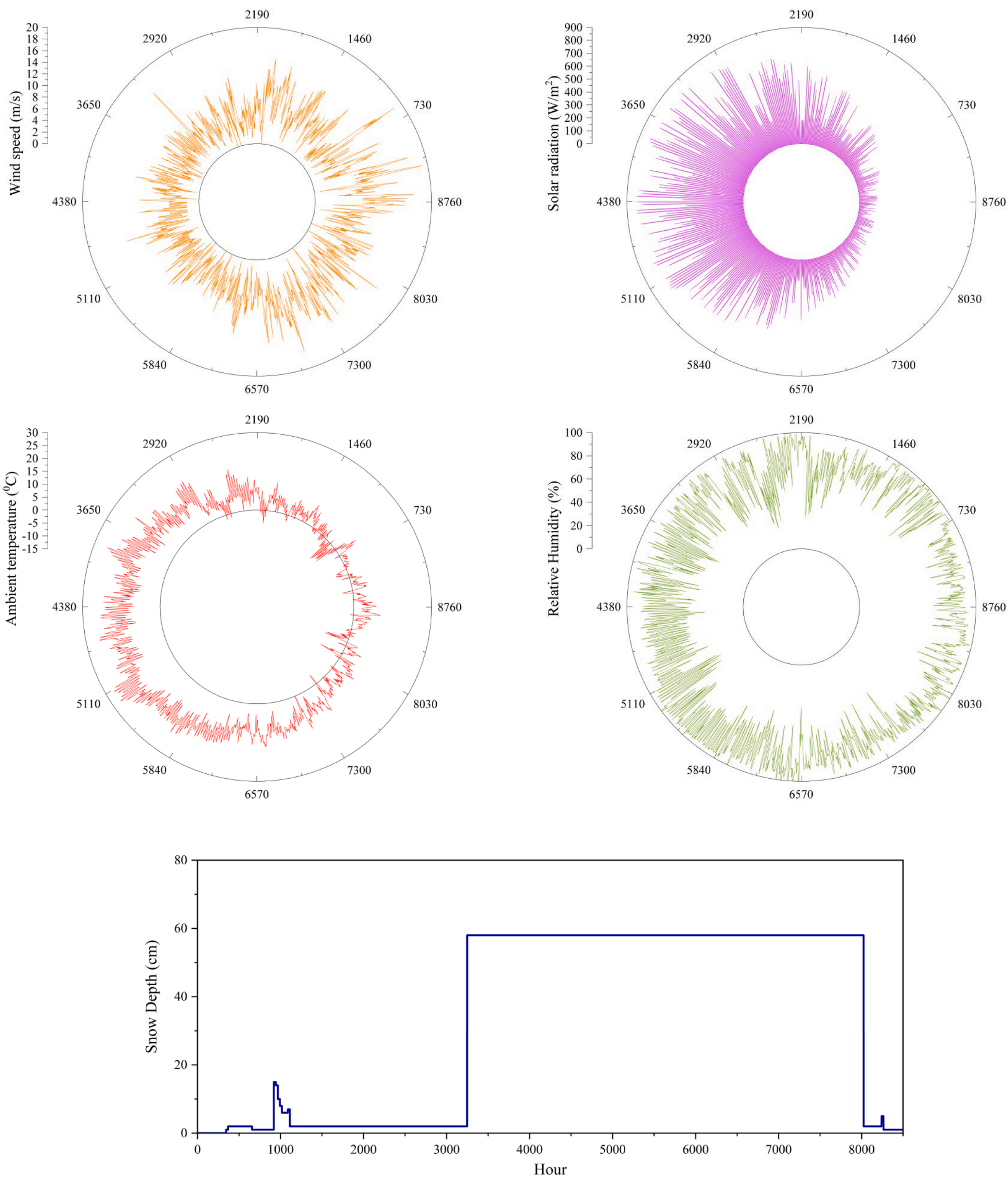

Fig. 3. Hourly variations in the Copenhagen city weather throughout a year.

indicate that the ambient temperature ranges from −15 °C to 30 °C, making Copenhagen one of the coldest regions in the world. This extreme cold climate necessitates a substantial heating load for the building. Copenhagen is considered a high-potential wind region, with wind speeds fluctuating between 0 and 20 m/s throughout the year, as shown in Fig. 3. The city also experiences significant snowfall, which contributes to the increased heating demands of the building. In summary, the analysis of these weather parameters highlights the challenges

Building	North	South	West	East
Windows	Low-E, Triple, Non-metal, Arg, H-Gain	Back Windows=High-SHGC	Clear, Double, Non-metal, Air, H-Gain	Clear, Double, Metal, Air
Window Areas	15% F25 B25 L25 R25	15%F20 B40 L20 R20	F18 B15 L15 R15	F18 B18 L18 R18
Door	Fiberglass	Fiberglass	Fiberglass	Steel
Door Areas	20 ft2	30 ft2	20 ft2	20 ft2
Wall Sheathing	R-5XPS	R-6 Polyiso	R-6 Polyiso	R-15XPS
Exterior Finish	Aluminum, Light	Aluminum, Medium/Dark	Brick, Light	Brick, Medium/Dark
Interzonal Walls	R-23 Closed Cell Spray Foam, 2*4, 16 in o.c.	R-13 Opened Cell Spray Foam, 2*4, 16 in o.c.	R-13 Opened Cell Spray Foam, 2*4, 16 in o.c.	R-13 Fiberglass Batt, 2*4, 16 in o.c.
Wood Stud	R-13 Cellulose, 2*4, 16 in o.c.	R-23 Closed Cell Spray Foam, 2*4, 16 in o.c.	R-13 Fiberglass Batt, 2*4, 16 in o.c.	R-20 Open Cell Spray Foam, 2*4, 16 in o.c.
Double Wood Stud	R-39 Cellulose, Gr-1, 2*4 Staggered, 24 in o.c.	R-45 Fiberglass, Gr-1, 2*4 Centered, 24 in o.c.	R-33 Fiberglass Batt, Gr-1, 2*4 Centered, 24 in o.c.	R-33 Fiberglass Batt, Gr-1, 2*4 Staggered, 24 in o.c.
Steel Stud	R-19 Fiberglass Batt, 2*6, 24 in o.c.	R-21 Fiberglass Batt, 2*4, 24 in o.c.	R-19 Fiberglass Batt, 2*6, 24 in o.c.	R-15 Fiberglass Batt, 2*4, 24 in o.c.
Interior Shading	Summer=0.6, winter=0.7	Summer=0.7, winter=0.95	Summer=0.7, winter=0.7	Summer=0.7, winter=0.7
Eaves	2 ft	3 ft	2 ft	2 ft
Overhangs	2 ft, Frist Story, Left Windows	2 ft, All Stories, All Windows	2 ft, All Stories, All Windows	2 ft, Frist Story, All Windows
Floor Mass	2 in, Gypsum Concrete	2 in, Gypsum Concrete	2 in, Gypsum Concrete	2 in, Gypsum Concrete
Exterior Wall Mass	2*5.8 in, Drywall	2*5.8 in, Drywall	PCM Drywall	PCM Drywall
Partition Wall Mass	2*5.8 in, Drywall	2*5.8 in, Drywall	2*5.8 in, Drywall	2*5.8 in, Drywall
Ceiling Mass	Drywall/PCM Mat	Drywall/PCM Mat	PCM Drywall	Drywall/PCM Mat
Carpet	80% Carpet	40% Carpet	60% Carpet	40% Carpet
Finished Roof	R-47.5 SIPs	R-38 Fiberglass Batt, 2*10	R-47.5 SIPs	R-30+R-19 Fiberglass Batt
Roof Material	Asphalt Shingles, Light	Metal, Light	Galvanized Steel	Galvanized Steel
Lighting	80% CLF	60% CLF	100% LED,Low efficacy	100% LED,Low efficacy
Pier & Beam	Ceiling R-13 Closed Cell Spray Foam	Ceiling R-13 Fiberglass Batt	Ceiling R-13 Fiberglass Batt	Ceiling R-13 Fiberglass Batt

Fig. 4. Optimum Building materials.

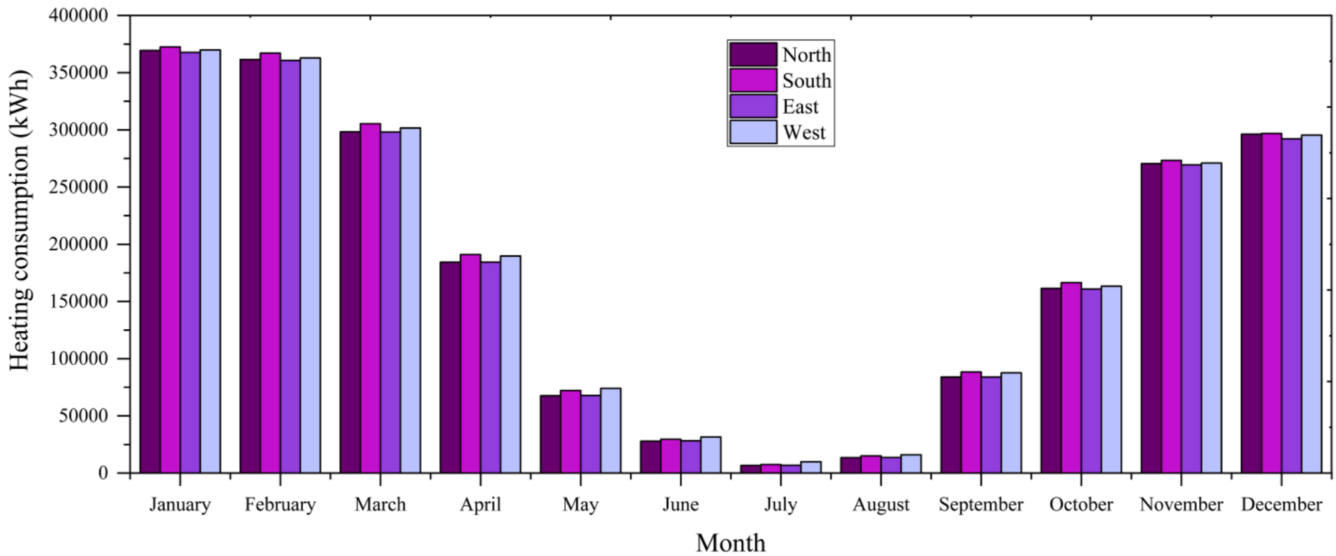

Fig. 5. Amount of heating bar consumed throughout the year.

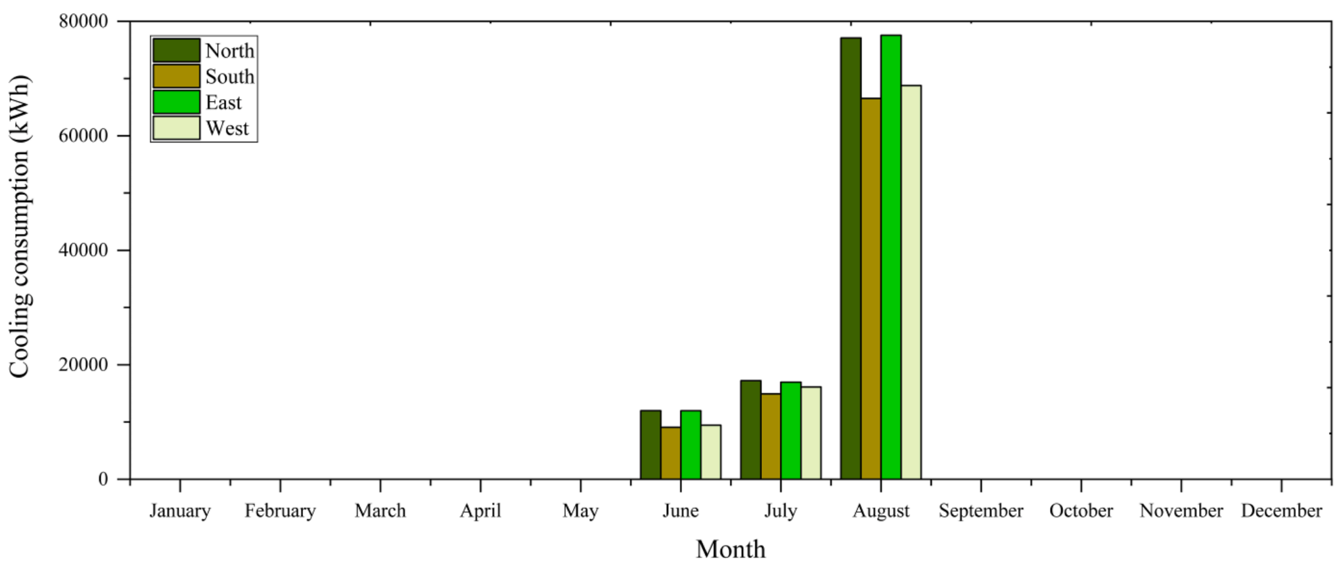

Fig. 6. Amount of cooling bar consumed throughout the year.

faced by residential buildings in Copenhagen due to the extreme cold climate, high heating requirements, and the impact of solar radiation, wind, and snowfall on energy consumption. Designing buildings that can effectively adapt to these environmental conditions is crucial for achieving energy efficiency and occupant comfort in Copenhagen's unique climate.

In designing the residential building in Copenhagen, various sizes and materials were selected to optimize its construction, with the goal of identifying the most effective structural solutions. Utilizing the BEopt optimization method, the study evaluated different materials and design features to determine the best combinations for energy efficiency and performance. Fig. 4 illustrates the optimal materials and characteristics identified for the building.

A few points should be made about optimizing energy consumption and building construction:

1- Modeling is done with BEopt (Building Energy Optimization Tool) software. (BEopt software is a tool for energy optimization in the building, which is used to evaluate the building and provide solutions to improve efficiency with the lowest cost. In BEopt, simulation is done based on the dimensions, type of materials, climate of the city of the building, and the direction of the building)
2- The important advantages of BEopt is adding materials or types of materials to the library or archive that are being introduced and are not available in the BEopt library.
3- The construction materials used, which are presented in Fig. 4, are located in the BEopt library.
4- BEopt optimization is done by choosing different materials for doors, windows, walls, ceilings, lamps, etc.
5- The different materials are selected for different parts of the building and problem solving begins. It takes hours to solve the problem according to the number of materials and the characteristics of the computer.
6- The selected materials and their number in this research were between 4 and 7 materials for different parts of the building (doors, windows, walls, ceilings, lamps, etc.).
7- The optimization is done by BEopt software and finally, the best and most optimal materials are selected among the selected materials

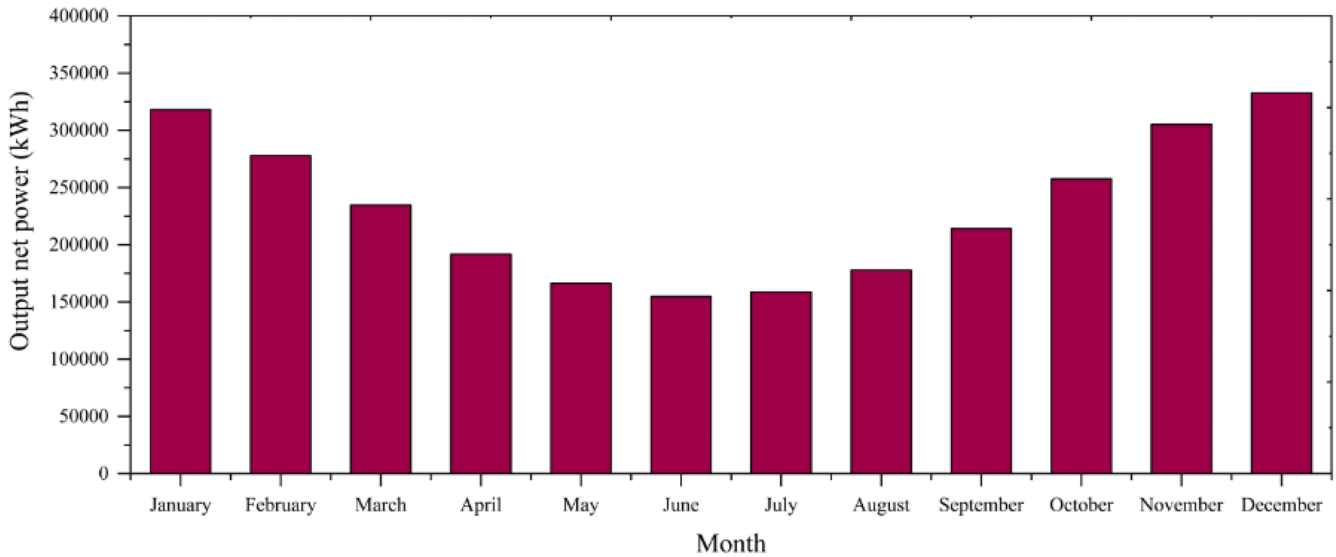

Fig. 7. Total amount of electricity used in a given year.

Table 1
The total annual energy consumption of the residential building.

Energy consumption	North	South	East	West
Electricity (kWh)	2789,416			
Cooling (kWh)	106,270.2	90,511.45	106,465.7	94,333.63
Heating (kWh)	2141,172	2184,980	2133,357	2172,425

Table 2
The best value for lowering CO_2 levels and conserving energy in the building.

Parameter	North	South	East	West
Energy Related Cost ($)	68,382.9	68,394.27	68,314.29	68,379.77
Energy Related Cost ($/yr)	1808.09	1808.68	1804.59	1807.93
Net Present Value ($)	280.17	34,284.01	287.19	267.23
Source Energy Saving (%/yr)	0.10	0.02	0.12	0.039
CO_2 Emission (Metric tons/ yr)	10.86	10.86	10.82	10.85
Site Energy Saving (%/yr)	0.12	0.03	0.15	0.05
CO_2 Saving (%/yr)	0.09	0.02	0.09	0.82

according to the goal of the problem, which is to reduce energy consumption.

8- Sequential search optimization technique is used by BEopt, which aims to:
   It finds construction plans with minimum cost at different levels of energy saving.
   It identifies several nearly optimal designs along the way, the aim of the research is to introduce the most optimal method. So, the optimization technique of this software is a sequential search among the selected materials to find the most optimal method.
9- The selected materials are optimal compared to other selected materials suitable for the climate of the study city and were found by the BEopt software, the monthly results of using the optimal materials are described in the text of the manuscript.

To assess the building's heating and cooling energy consumption throughout the year, the orientation of the structure was analyzed in four directions: north, south, east, and west. The energy consumption patterns for each orientation were compared to identify the most optimal placement. Fig. 5 presents the monthly and annual heating load consumption of the 5-story, 10-unit residential building in the four different orientations. The results show that the building's heating energy consumption fluctuates between 0 and 375,000 kWh over the course of the year. Due to the extreme cold air temperatures in Copenhagen, the building requires a significant heating load, regardless of its orientation.

Fig. 6 illustrates the monthly cooling load consumption for the 5-story, 10-unit residential building over the course of one year, analyzed from four different orientations. The cooling energy consumption in this study shows a range from 0 to 80,000 kWh throughout the year. This relatively low cooling load requirement is attributed to the cooler air temperatures prevalent in the region.

Fig. 7 displays the monthly electricity consumption of the building over the course of one year. electricity utilized for lighting & other purposes in the residential building fluctuates between 1500,000 and 4000,000 kWh annually and on a monthly basis.

Table 1 presents a comparison of the total annual energy consumption for a 5-story residential building optimized across four orientations: **north, south, east, and west**. The data highlights the differences in energy usage based on the building's directional placement.

The findings reveal that the optimal orientation for minimizing cooling energy consumption is the south, followed by west, north, and east. Conversely, the lowest heating energy demand is observed in the east, north, west, and south orientations, respectively. Table 2 provides a comprehensive analysis of the cost, energy consumption, and CO2 emissions associated with four different approaches to residential building construction in Copenhagen. This comparative assessment offers valuable insights into the environmental and economic implications of each method.

3. System analysis

3.1. System description

The schematic diagram of the proposed geothermal power plant system is shown in Fig. 8. This system is designed to harness geothermal energy and consists of geothermal well subsystems, a modified ORC utilizing an organic working fluid, and a heat exchanger. In this system, a new design of the modified organic Rankine cycle is used using heat recovery steam generator equipment, ejector, and preheater. An ejector is a device that can remove fluid flows by creating suction in an environment and creating a vacuum in the system. A preheater is a device designed to heat the fluid flow before another process. A heat recovery vapour generator is a type of boiler that uses the thermal energy of a process to produce hot steam and in fact, recovers the energy contained

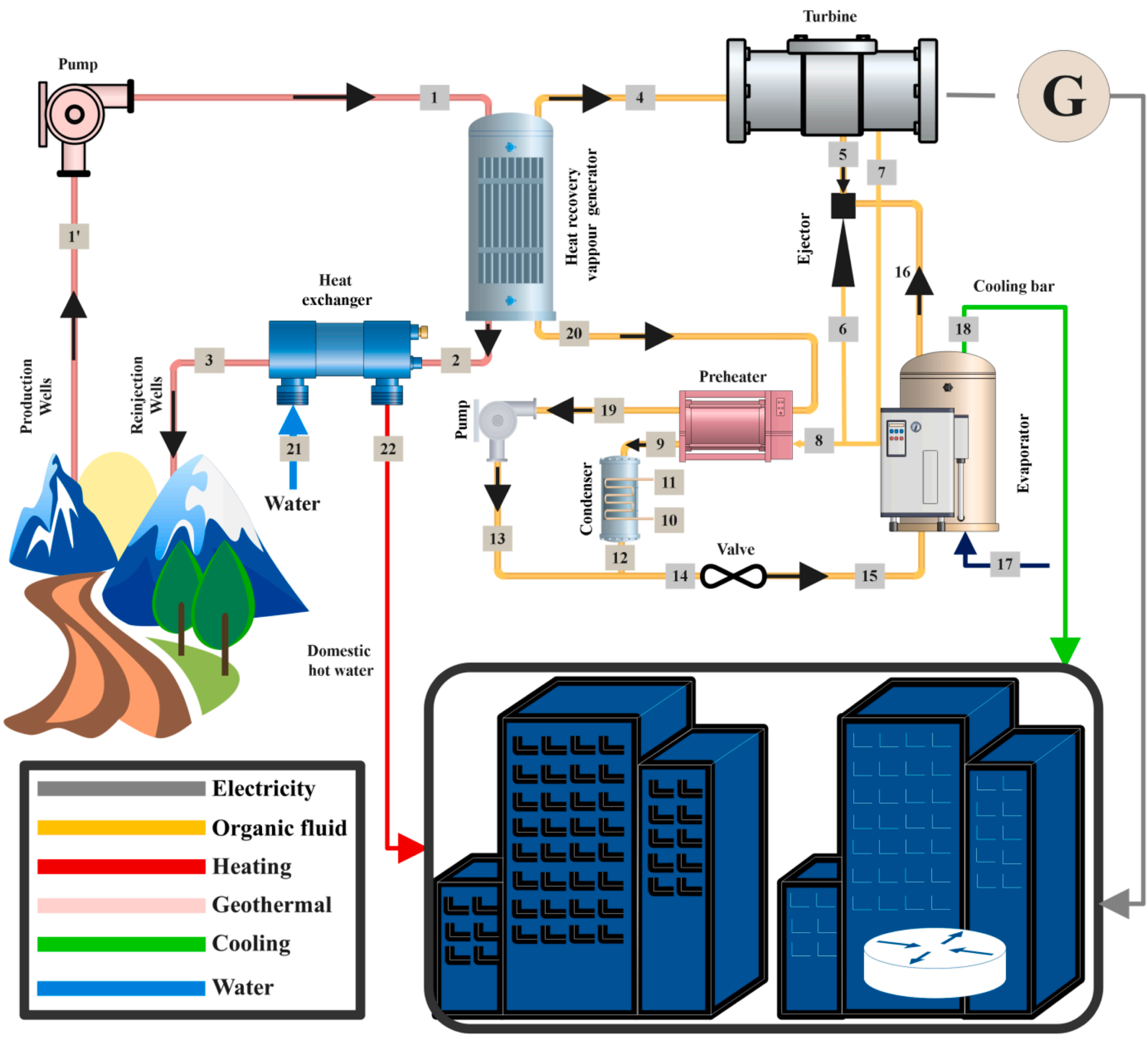

Fig. 8. Schematic of the proposed system.

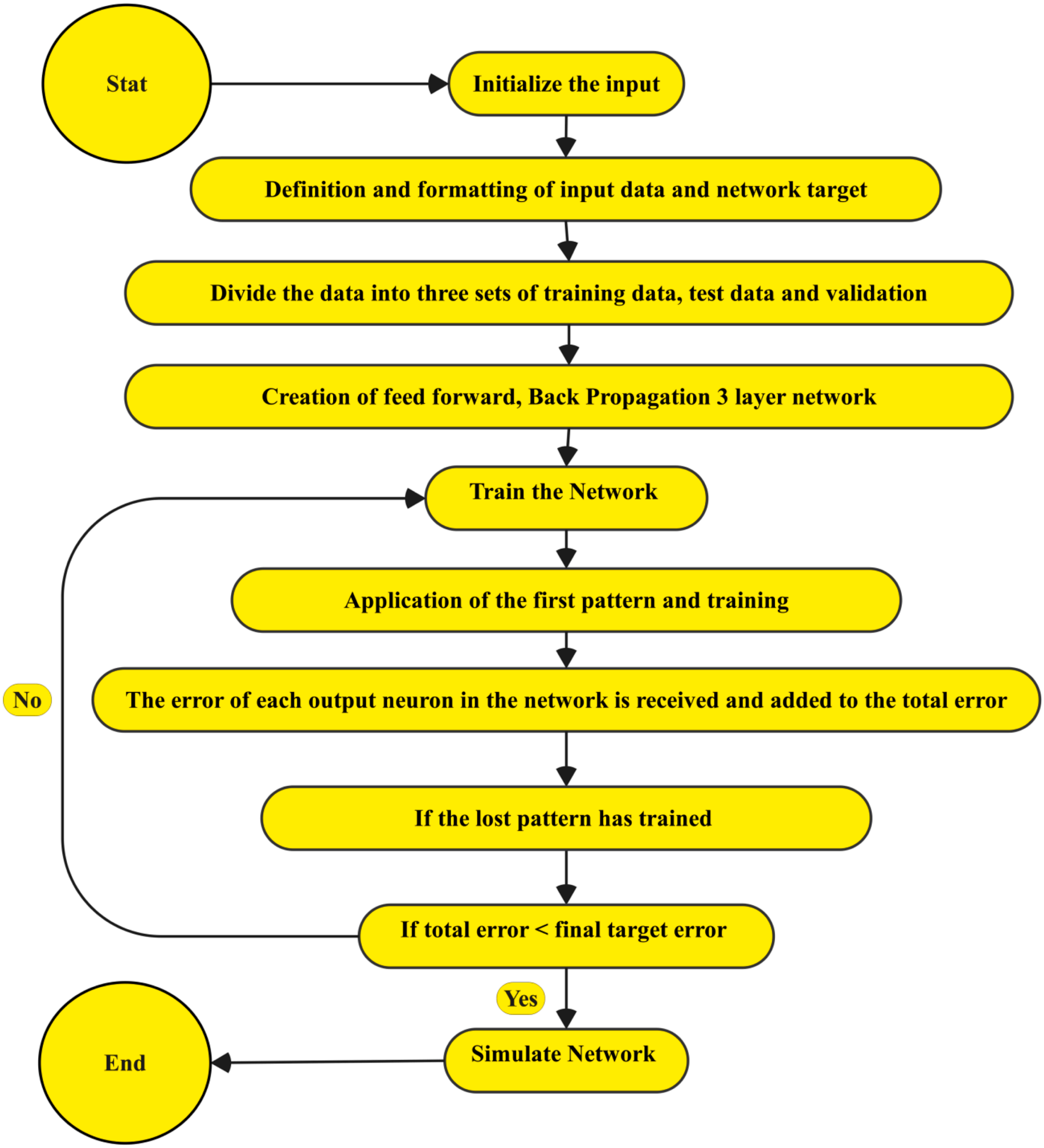

Fig. 9. Neural network flowchart.

in the combustion products. The primary purpose of this proposed co-generation system is to generate electricity (output power), provide cooling bar, and produce hot water for heating applications. The system operates by utilizing a low-temperature heat source to drive the turbine. In this case, geothermal energy, extracted from the geothermal reservoir, serves as the heat source. The extracted heat is fed into the heat recovery generator, where it undergoes a cyclic process. At the final stage, the heat is re-injected back into the ground. A pump, located before point 1, is responsible for circulating the fluid from the geothermal reservoir into the system. Since the inlet and outlet fluid pressures remain constant, there is no need for phase change, and the pump's power consumption is negligible. The fluid, pumped from the geothermal reservoir, enters the ORC and drives the turbine to generate electricity. The heat is then transferred to the ORC evaporator, where it is used to produce the cooling load for the building's cooling requirements. Finally, the heat exchanger utilizes the energy returned to the ground to generate hot water, which can be used for heating purposes in the residential building. This integrated approach ensures the efficient utilization of geothermal energy, minimizing waste and maximizing the system's overall effectiveness in meeting the building's

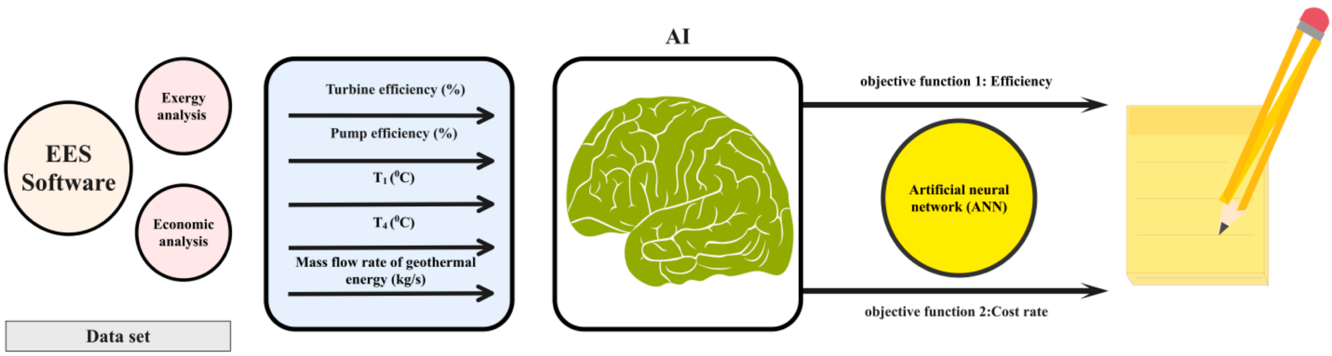

Fig. 10. AI structure.

Table 3
Validation.

Terms	Present model	Amiri rad et al.	Error (%)
Temperature Source (°C)	150	150	–
Mass flow (kg/s)	15	15	–
Inlet pressure turbine (bar)	27.30	27.3	–
Turbine power (kW)	120.4	121.8	1.1
Output power (kW)	106.8	105.8	0.94
Thermal efficiency (%)	7.8	7.7	0.7

Table 4
Range of optimization variables.

Parameter	Lower limit	Upper limit
Turbine efficiency (%)	0.7	0.95
T_4 (K)	380	450
T_1 (K)	460	520
Pinch point (°C)	5	15
Pump efficiency (%)	0.7	0.95
Mass flow rate (kg/h)	5	20

energy demands.

3.2. Cogeneration system (Optimization with AI)

Artificial Intelligence Neural Networks (ANNs) are a subset of machine learning models inspired by the structure and function of neurons in biological organisms. An ANN consists of a network of interconnected nodes, referred to as artificial neurons. If we liken the artificial intelligence model to a brain, the neural pathways and processing nodes that facilitate the information processing are known as artificial intelligence neural networks [26–28]. Fig. 9 illustrates the flowchart depicting the neural network methodology.

The output data generated from the proposed co-generation system are utilized as inputs for Artificial Neural Networks (ANNs). These outputs encompass various performance metrics, including energy production levels, efficiency rates, and operational parameters of the co-generation system. By feeding this data into the ANN, the model is trained to recognize patterns and relationships within the data, ultimately leading to the development of a mathematical equation or model that accurately represents the system's behavior. Once the ANN has produced this mathematical model, it serves as a crucial input for the multi-objective optimization (MOO) process. This process aims to identify the best possible configurations and operational strategies for the co-generation system, balancing multiple objectives such as maximizing energy output, minimizing costs, and reducing environmental impact. The mathematical model derived from the ANN allows for the simulation of various scenarios and conditions, enabling decision-makers to explore different strategies and their potential outcomes. By integrating the ANN-generated model into the optimization framework,

Table 5
Optimal values of decision variables.

Decision variables	points	N
Pump efficiency (%)	0.8226	300
Turbine efficiency (%)	0.8238	300
Pinch point (°C)	10.0013	300
Mass flow rate	12.1843	300
T_1 (°C)	489.0511	300
T_4 (°C)	414.5602	300

the research can effectively evaluate trade-offs between competing objectives, leading to more informed and efficient design choices. In summary, the synergy between the output data from the co-generation system, the ANN's mathematical modeling, and MOO process creates a robust framework for enhancing the performance and sustainability of the co-generation system. This approach not only improves operational efficiency but also contributes to the broader goals of energy conservation and environmental stewardship. Fig. 10 shows the structure of the AI process.

4. Results and discussion

4.1. Validation

Before the discussion system was analyzed, a validation procedure was put in place to guarantee the validity of the results and support the work done. Specifically, the performance of the Organic Rankine Cycle (ORC) was validated by comparing the results of the present study with those of Amiri Rad et al. [29]. Table 3 presents a detailed comparison of the results from both studies. The data clearly indicate that the outcomes of the current research align closely with those reported in the reference study, demonstrating a high level of accuracy in the model employed in this analysis. This validation process is crucial as it not only reinforces the credibility of the findings but also ensures that the methodologies applied are robust and reliable. By confirming that the results are consistent with established research, we can confidently proceed with the subsequent discussions and analyses, knowing that they are built upon a solid foundation of validated data. This step is essential for establishing the relevance and applicability of the research in practical scenarios, further enhancing its contribution to the field of study.

Table 6
Optimal value of objective functions.

Objective functions	N	Optimum point	Minimum	Maximum
Exergy efficiency (%)	300	63.79485	44.01000	86.87000
Cost rate ($/h)	300	57.82670	26.66000	97.68000

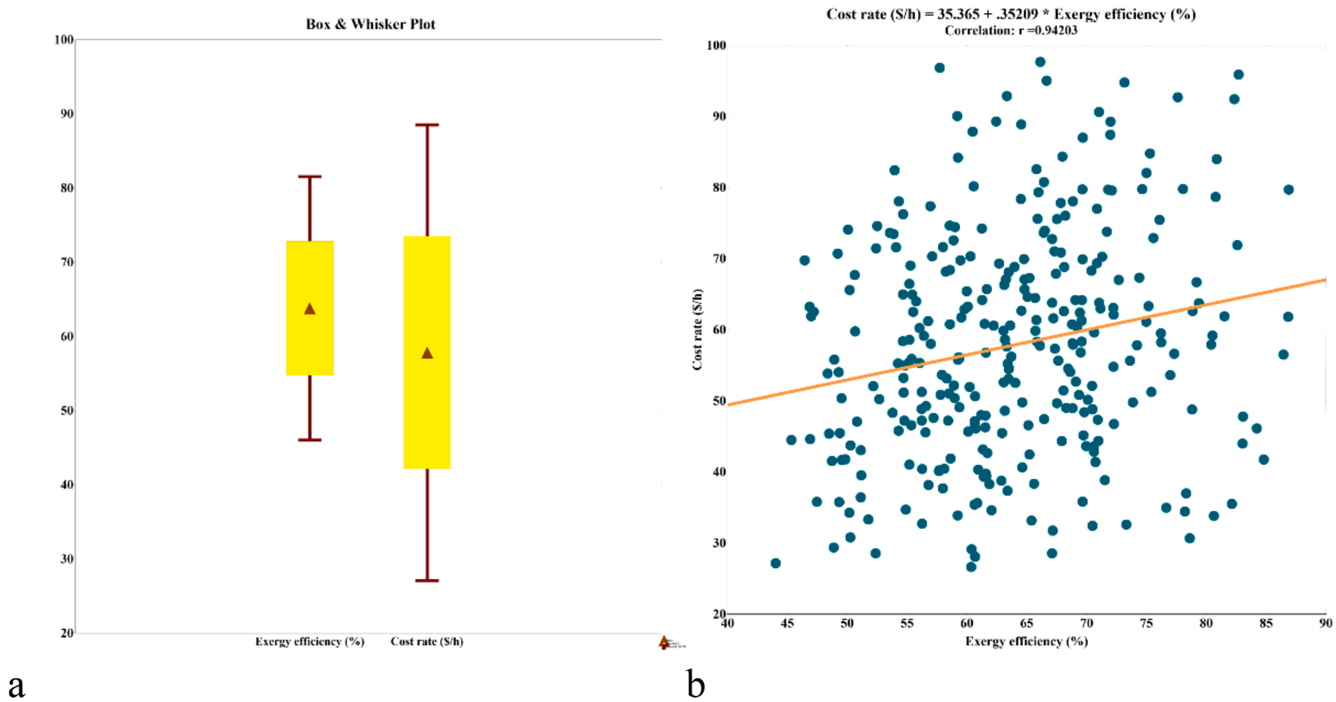

Fig. 11. Limited variations of objective functions (a) and Pareto chart (b).

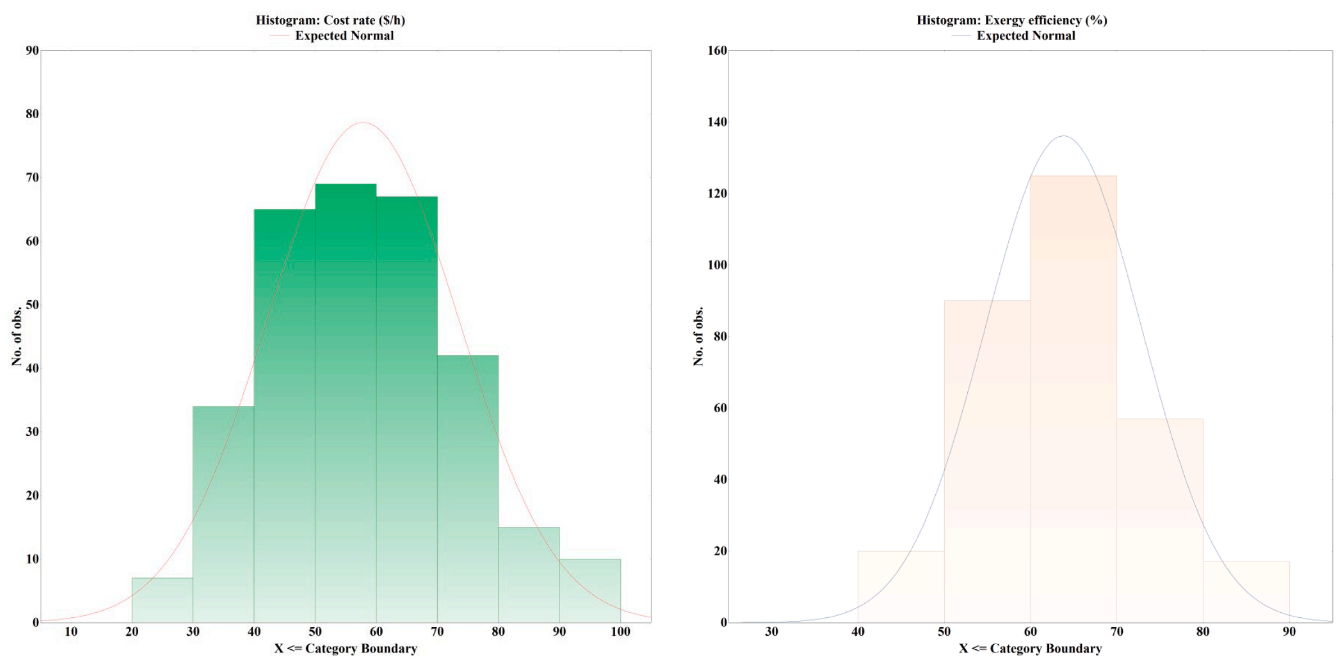

Fig. 12. Histogram diagram showing the two function targets that are being studied.

4.2. Optimization results

Multi-objective optimization, employing the neural network method, was conducted to enhance the performance and reduce the costs associated with the system. The optimization process aimed to simultaneously increase exergy efficiency and minimize the cost rate, thereby improving the overall viability and sustainability of the system. Table 4 outlines the optimization variables and their respective ranges. These variables represent the key parameters that can be adjusted to achieve the desired outcomes, such as maximizing exergy efficiency and minimizing cost rates. By defining the appropriate ranges for each variable, the optimization algorithm can explore a wide solution space, increasing the likelihood of identifying the most optimal configurations. The neural network method serves as a powerful tool in this optimization process. By leveraging artificial neural networks, the algorithm can learn from the input data and generate accurate predictions of the system's output indicators under various scenarios. This predictive capability is crucial in the optimization process, as it allows for the rapid evaluation of numerous scenarios without the need for extensive experimental testing or simulations. By integrating the neural network method with multi-objective optimization techniques, the research can effectively navigate the trade-offs between competing objectives, such

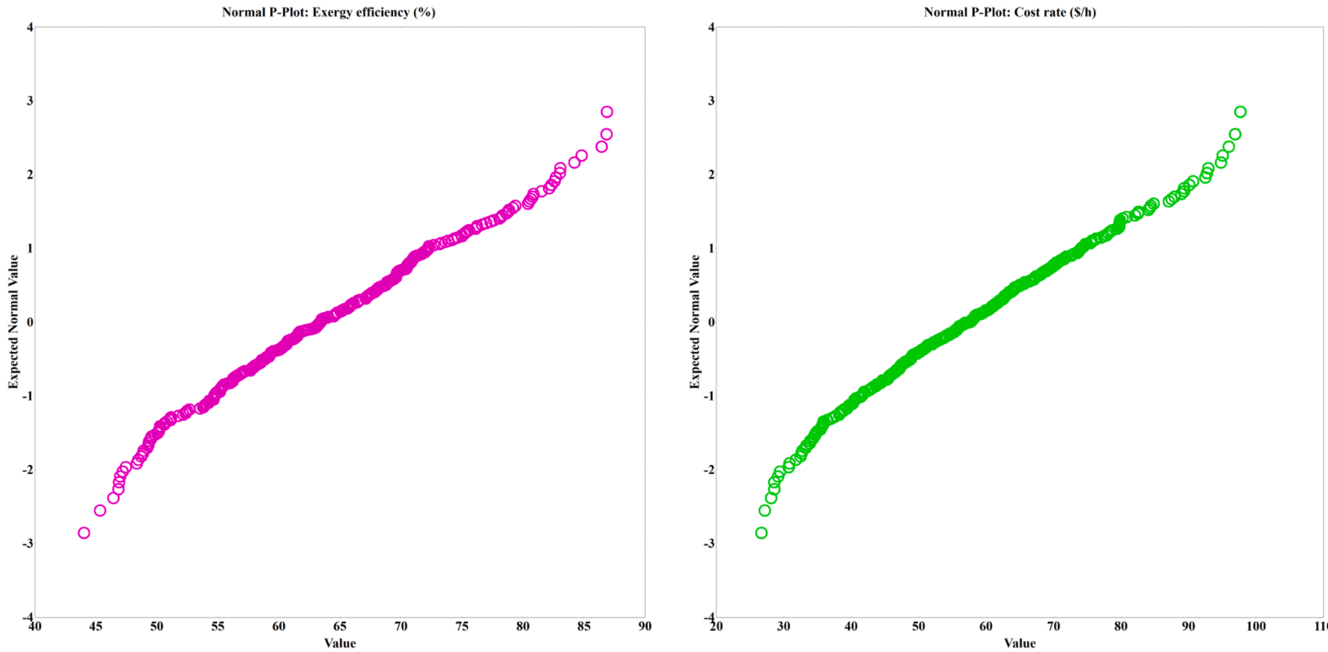

Fig. 13. Normality diagram of objective functions.

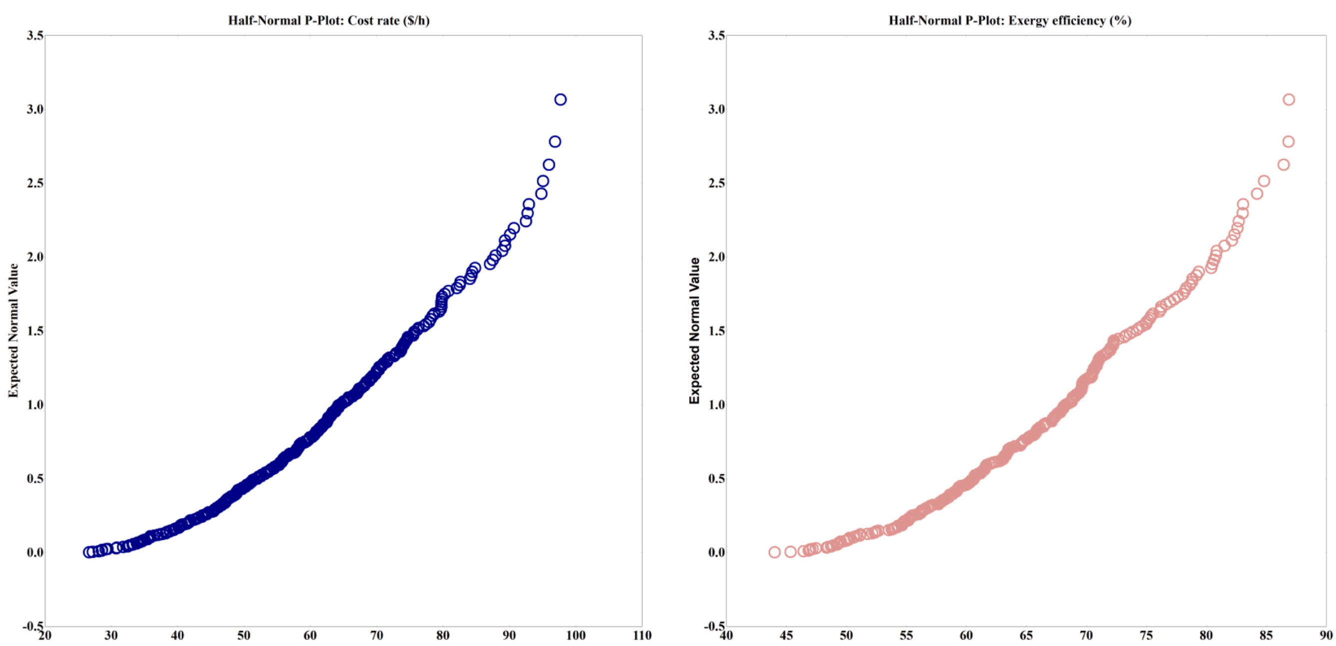

Fig. 14. Forecasting the two goal functions that are being studied's flow functions.

as efficiency and cost. The resulting optimized solutions provide valuable insights into the design parameters and operational strategies that can maximize the system's potential while minimizing its economic and environmental impact. This approach not only enhances the performance of the specific system under study but also contributes to the broader field of energy systems optimization. The methodologies and insights gained from this research can be applied to a wide range of energy systems, fostering the development of more efficient, cost-effective, and sustainable solutions for energy generation and distribution.

The primary goal of this optimization process is to enhance the technical parameters of new proposed co-generation system, particularly focusing on increasing exergy efficiency while simultaneously reducing overall system costs. This dual objective is crucial for improving the system's performance and ensuring its economic viability. Tables 5 and 6 provide a summary of the optimal values for the decision variables and the corresponding objective functions achieved through the optimization process. These tables highlight the specific parameters that were adjusted to attain the most favorable outcomes, offering a clear view of how the optimization has impacted the system's design and functionality. In this research, the necessary data was extracted from the modeling solutions of the system, which served as the foundation for the optimization process. The neural network method was employed to analyze this data effectively. By inputting the relevant information into the neural network, the model was able to learn from the existing data patterns and relationships, facilitating a more informed

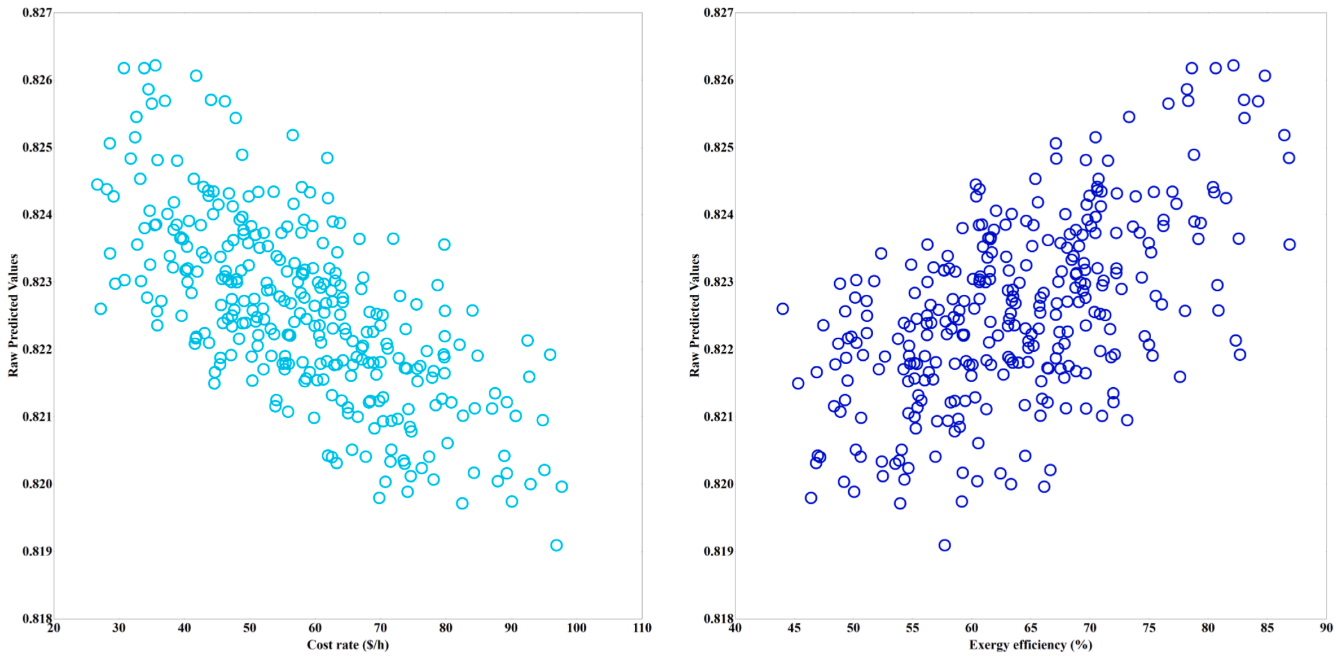

Fig. 15. Raw predicted values of functions.

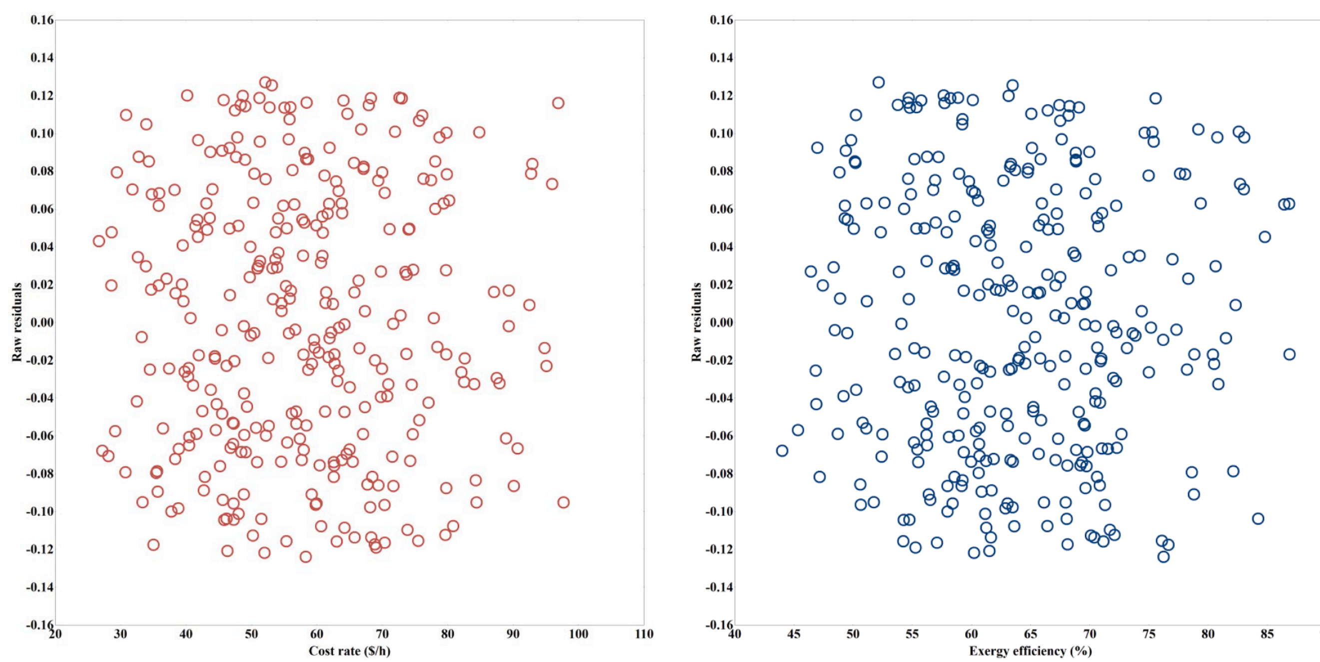

Fig. 16. Raw residual values of functions.

optimization process. Subsequently, the optimization was carried out using meta-heuristic algorithms, which are designed to efficiently explore the solution space and identify optimal configurations. These algorithms are particularly effective for complex optimization problems, as they can navigate through numerous potential solutions while balancing multiple objectives. Overall, this integrated approach—combining neural networks with meta-heuristic optimization techniques—enables a comprehensive analysis of the system. It not only enhances the technical performance of the system by improving exergy efficiency but also contributes to cost reduction, making the system more competitive and sustainable in the long run. The methodologies developed in this research can be applied to various energy systems, paving the way for future advancements in energy efficiency and optimization.

The most ideal value for the objective functions is chosen, and the limit of modifications for the objective functions is shown in Fig. 11(a). Additionally, the Pareto diagram showing the trade-offs between the 2 objective functions (OFs) taken into account in the MOO process is shown in Fig. 11(b). The Pareto diagram is an effective tool for illustrating the best possible outcomes that concurrently achieve several, frequently incompatible goals. In this research, the multi-objective optimization problem involves two competing objective functions that need to be minimized or maximized simultaneously. These objective functions, such as maximizing exergy efficiency and minimizing system

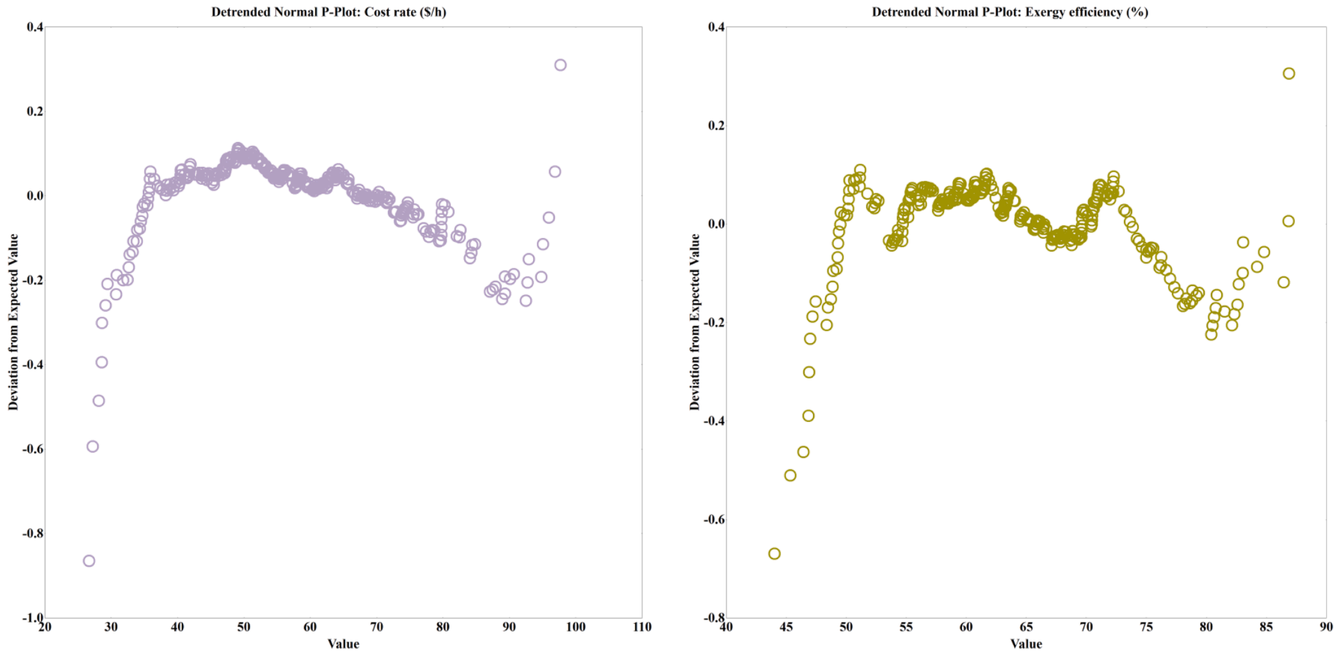

Fig. 17. Deviation from expected values of functions.

costs, are inherently conflicting in nature. Improving one objective function may lead to a deterioration in the other, making it challenging to find a single optimal solution that satisfies both objectives equally. The Pareto diagram in Fig. 11(b) illustrates the set of Pareto optimal solutions, which represent the best possible trade-offs between the two objective functions. Each point on the Pareto front represents a solution that cannot be improved in one objective without sacrificing the other. These solutions are considered equally optimal, as they represent the best compromise between the competing objectives. By identifying the Pareto optimal solutions, decision-makers can gain valuable insights into the range of possible outcomes and make informed choices based on their preferences and priorities. The Pareto diagram helps to visualize the trade-offs and supports the selection of the most suitable solution for the specific application or context. In the context of this research, the Pareto optimal solutions provide a range of options that balance exergy efficiency and system costs. These solutions can be further analyzed and refined based on additional constraints or preferences, such as budget limitations, environmental regulations, or specific performance requirements. By employing multi-objective optimization techniques and leveraging the insights from the Pareto diagram, this research contributes to the development of more efficient, cost-effective, and sustainable energy systems. The methodologies and tools presented can be adapted and applied to various energy optimization problems, fostering innovation and progress in the field of energy systems design and operation.

Fig. 12 shows the histogram of the two target functions of η_{ex} and $\dot{C}_{tot}$, which are the two general answers for the two processes of training and calculation. The goal function's value is inserted on the horizontal axis, and the frequency % is displayed on the vertical axis.

In Fig. 13, the normality diagram of two objective functions of η_{ex} and $\dot{C}_{tot}$ of the geothermal power plant is obtained; this graph shows the normal probability of residuals obtained from linear regression analysis.

Fig. 14 examines the expected normal value for the two objective functions of η_{ex} and $\dot{C}_{tot}$.

The actual values of the 2 OFs, exergy efficiency (EE) and cost rate (CR), are contrasted with the raw anticipated values of OFs in Fig. 15 and Fig. 16 displays the amouts of the OFs' raw residuals in comparison to the two objective functions' actual values, η_{ex} and $\dot{C}_{tot}$. Furthermore, Fig. 17 discusses the lowered normal values in relation to the deviation values from the predicted value during the multi-objective optimization of the η_{ex} and $\dot{C}_{tot}$ objective functions.

Fig. 18 shows the changes in decision variables on the objective function of η_{ex}. The results of the investigations showed that out of the 6 decision-making variables examined on system performance, 4 variables have the highest effect on rising η_{ex} in optimal mode. Changes in geothermal energy and changes in organic turbine performance are known as the most influential parameters on system performance. The use of geothermal energy temperature, organic turbine input temperature, turbine efficiency, and evaporator pinch point temperature have the greatest effect on system efficiency. The changes in the objective function of efficiency in each range of the decision variable are represented by parametric analysis diagrams of design factors impacting the η_{ex} objective function, which are displayed as load distribution diagrams. The parametric study has been investigated in the optimization mode and by examining the simultaneous effect of all inputs on the objective function, which in addition to the parameter introduced in the horizontal axis of the graph, changes of 5 other parameters on η_{ex} have also been involved. Also, Fig. 19 shows the changes in decision variables on the $\dot{C}_{tot}$ objective function. Geothermal energy temperature, input temperature to the organic turbine, turbine efficiency, and evaporator pinch point temperature were identified as 4 decision variables influencing the economic performance of the system.

4.3. Economic analysis

The distribution of cost rates among the different system components is shown in Fig. 20. The components are categorized into two primary sections: the ORC unit and the heat exchanger. $\dot{C}_{tot}$ of operating the system is calculated to be $68.485 per hour. Within this framework, the ORC unit represents the most significant expense, accounting for $66.025 per hour, while the heat exchanger contributes a comparatively minor cost of $2.46 per hour. This indicates that the ORC unit is the primary driver of costs within the system. Among the various components of the ORC, the HRVG and the evaporator stand out as the most expensive elements, with cost rates of $20.06 per hour and $17.73 per hour, respectively. These high costs reflect the complexity and critical functionality of these components in the overall operation of the ORC system. In contrast, the ejector and pump have the lowest cost rates among the ORC equipment, indicating that these components are more

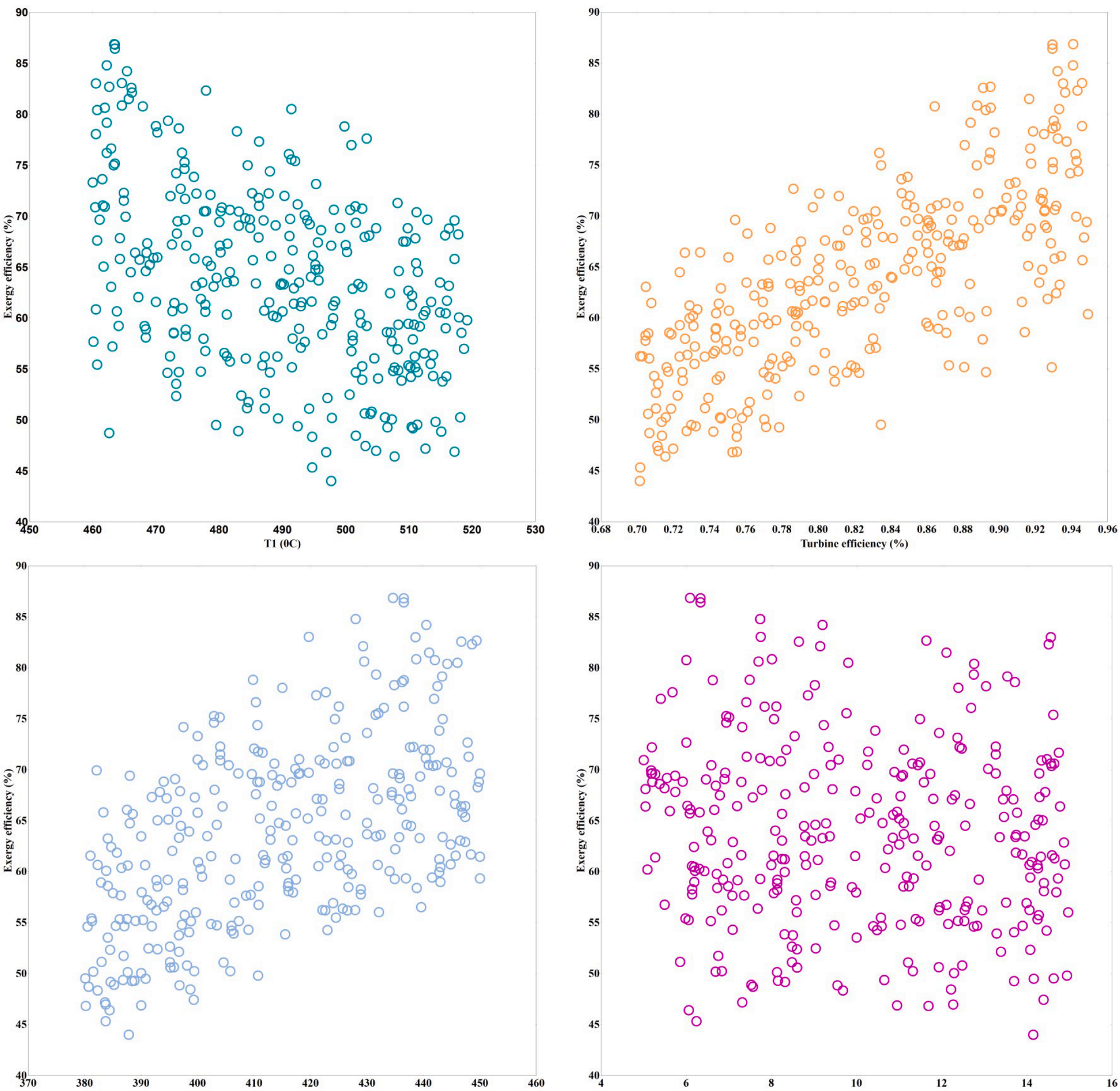

Fig. 18. Changes of decision variables on η_{ex}.

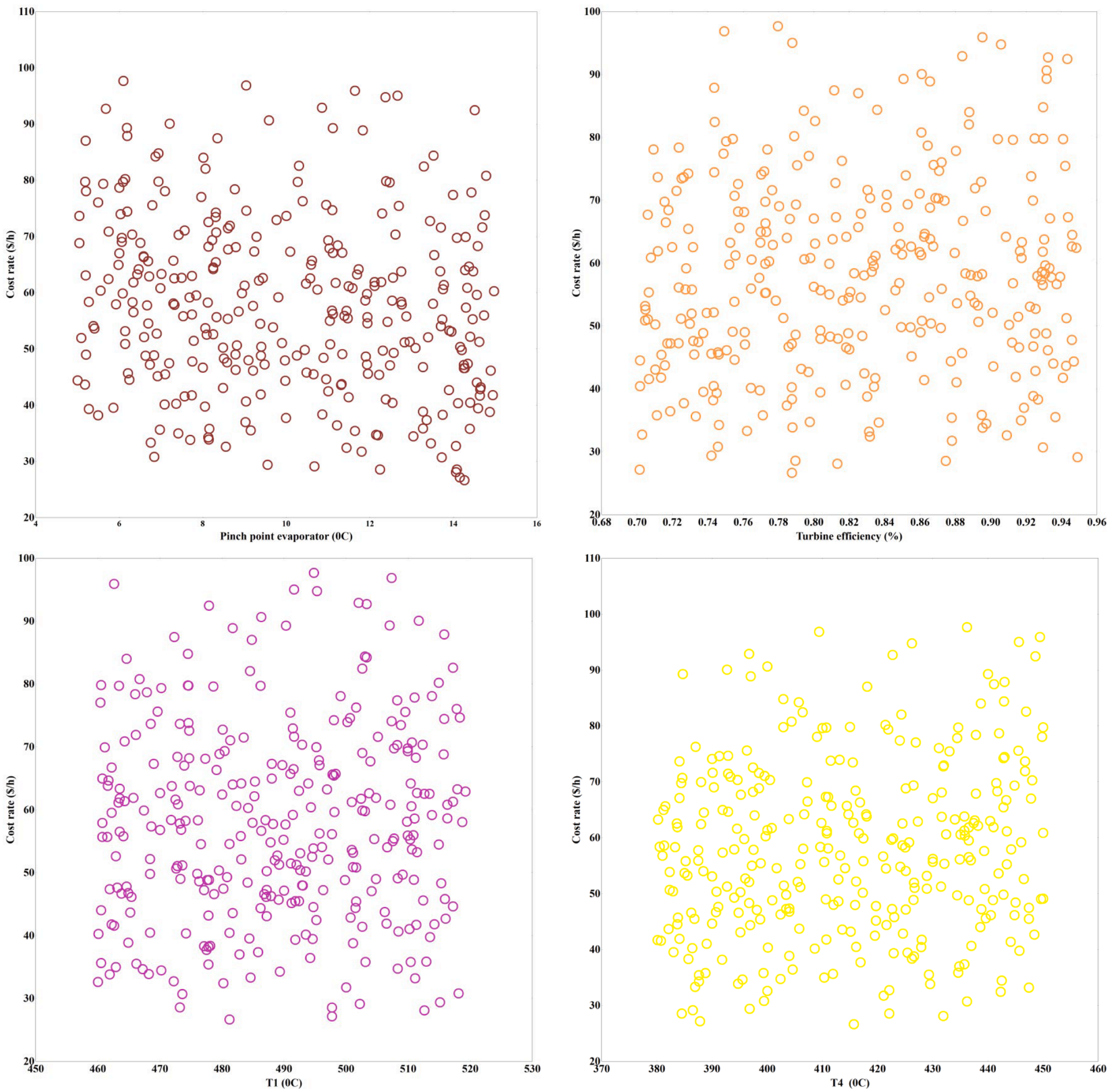

Fig. 19. Changes of decision variables on $\dot{C}_{tot}$.

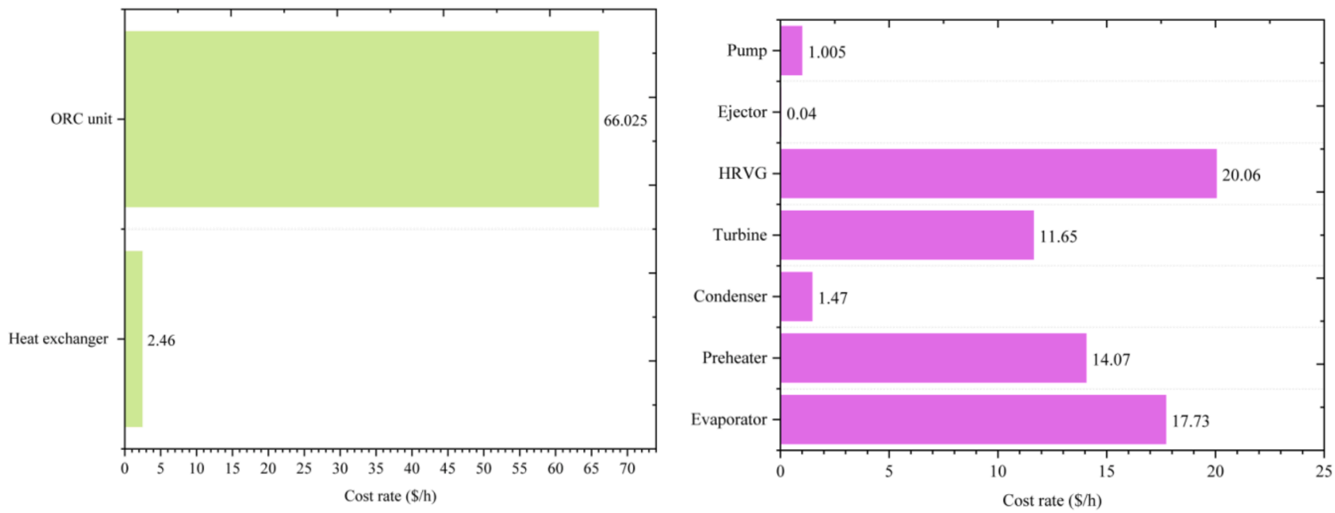

Fig. 20. System cost rate.

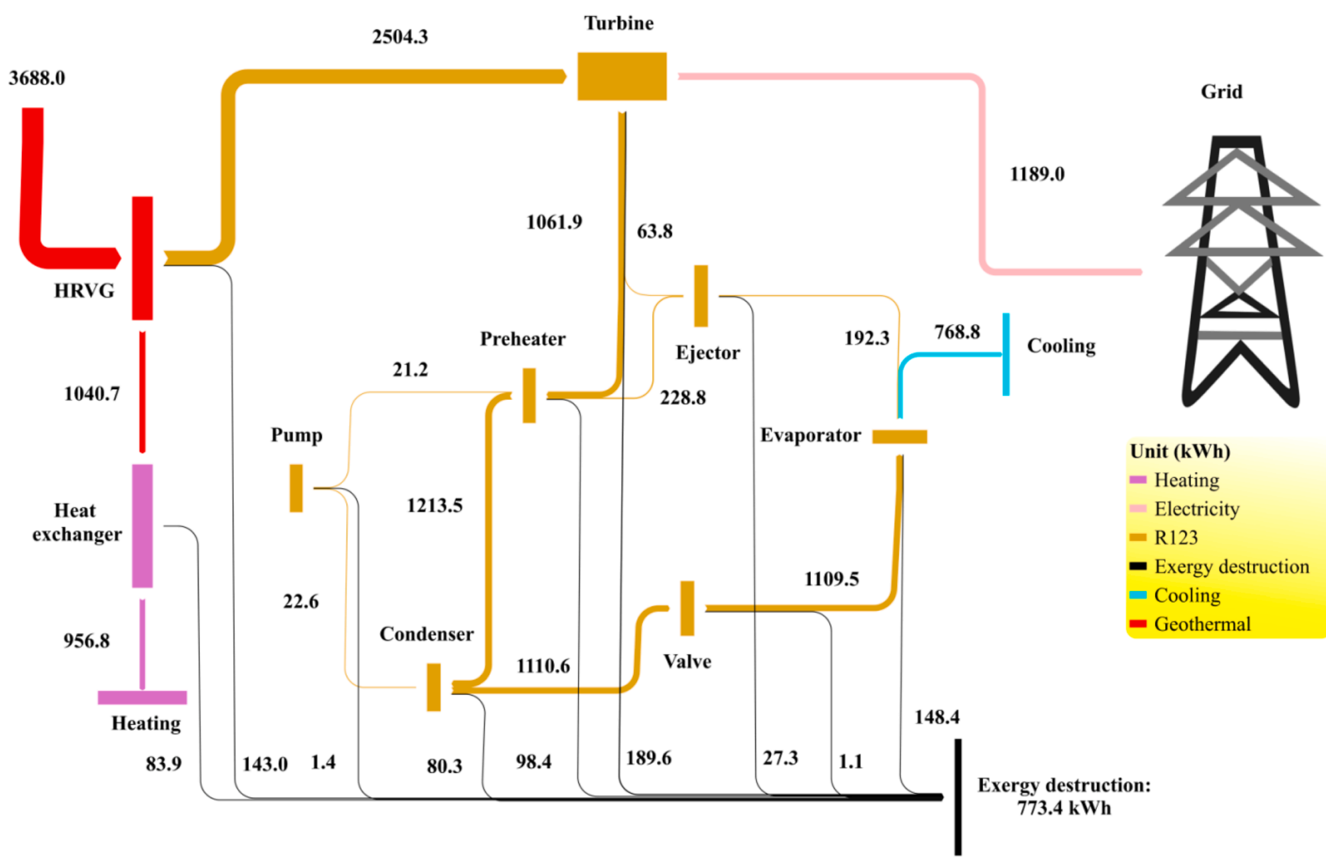

Fig. 21. Grossman diagram of the proposed system.

economical to operate. This cost distribution highlights the importance of considering both the initial investment and ongoing operational expenses when evaluating the economic viability of the system. Understanding the cost rate distribution of system components is essential for identifying areas where efficiency improvements can be made. By focusing on optimizing the more expensive components, such as the HRVG and evaporator, it may be possible to reduce overall system costs while maintaining performance. This analysis not only aids in cost management but also informs future design and operational decisions aimed at enhancing the economic sustainability of the system.

4.4. Exergy analysis

Exergy analysis serves as a crucial methodology for enhancing the understanding and performance of energy systems by identifying the primary sources of exergy degradation ($\dot{E}x_{dest}$). The Grossman diagram, illustrated in Fig. 21, is generated under optimal conditions and functions as a valuable tool for exergy analysis, visually representing the exergy rates of each stream alongside the $\dot{E}x_{dest}$ across all components. The analysis commences with an input exergy rate of 3688 kWh derived from the ground, which is subsequently directed into the HRVG

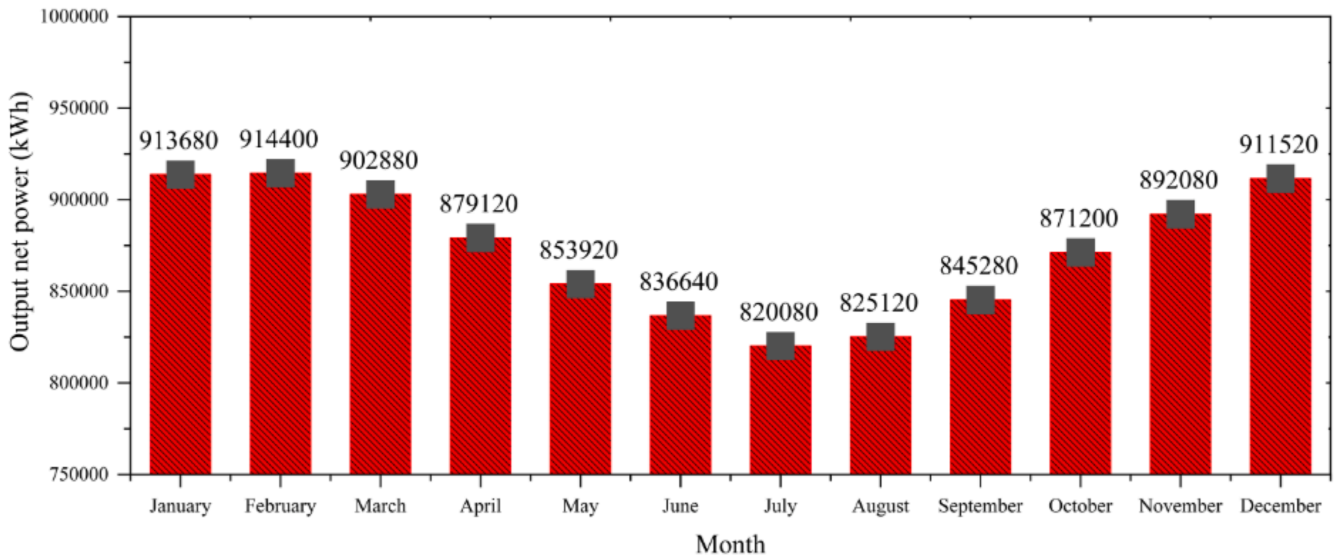

Fig. 22. System's net power generation rate.

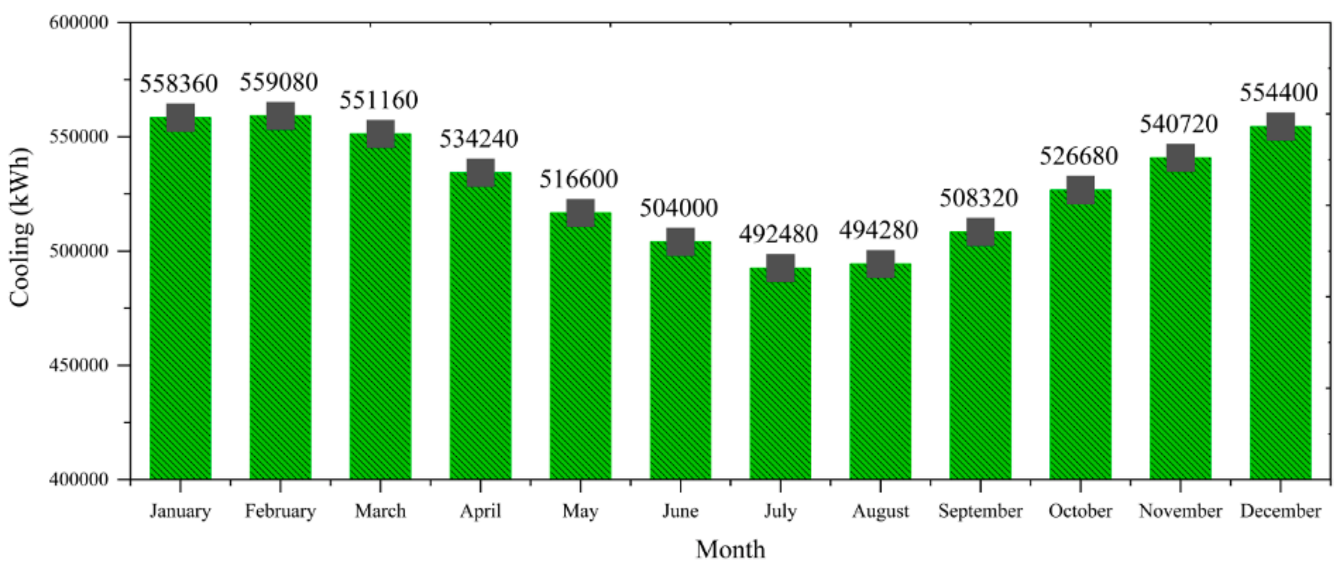

Fig. 23. The amount of monthly cooling production.

equipment. From this equipment, an exergy output of 2504 kWh is supplied to the ORC turbine, while an exergy loss of 143 kWh occurs within the HRVG. Additionally, the system transfers 1040.7 kWh of exergy to the heat exchanger, which experiences a loss of 83.9 kWh, ultimately producing 956.8 kWh of heating. The turbine further contributes to exergy losses amounting to 189.6 kWh. Moreover, the system incorporates an input of 192.3 kWh of exergy from the ejector and 1109.5 kWh from the condenser into the evaporator, which utilizes 768.8 kWh of heat output for cooling purposes. This comprehensive exergy analysis highlights the intricate interactions and losses within the system, providing insights for potential improvements in efficiency and performance. The exergy analysis conducted on the system revealed that the highest rates of $\dot{E}x_{dest}$ are associated with the turbine, evaporator, HRVG unit, preheater, heat exchanger, and condenser. In contrast, the equipment exhibiting the lowest rates of $\dot{E}x_{dest}$ includes the pumps and ejectors. The primary function of the pump within this system is to mechanically facilitate the movement of fluid, which accounts for its minimal $\dot{E}x_{dest}$. The system generates a total electrical output of 1189 kWh supplied to the power grid, while $\dot{E}x_{dest,tot}$ for the entire system amounts to 773.4 kWh.

4.5. Case study

This research examines the technical, economic, and environmental performance of a designed system in Denmark, with a focus on the city of Copenhagen. Copenhagen experiences comfortable and partly cloudy summers, while the winters are long, very cold, snowy, windy, and mostly cloudy. Throughout the year, temperatures typically range from −1.7 °C to 21.7 °C, rarely falling below −8.3 °C or exceeding 26.1 °C. The best time to visit Copenhagen for warm-weather activities is typically from late June to late August, based on the tourism score. Fig. 22 illustrates the changes in the net production power of the entire system in relation to variations in the monthly weather parameters for Copenhagen. The results indicate that as the ambient temperature increases and more heat is input to the ORC by the HRVG unit, the system's production power decreases during the warmer months of the year. The system's production capacity varies between 800,000 kWh and 920,000 kWh throughout the year.

Fig. 23 illustrates the monthly fluctuations in the production of

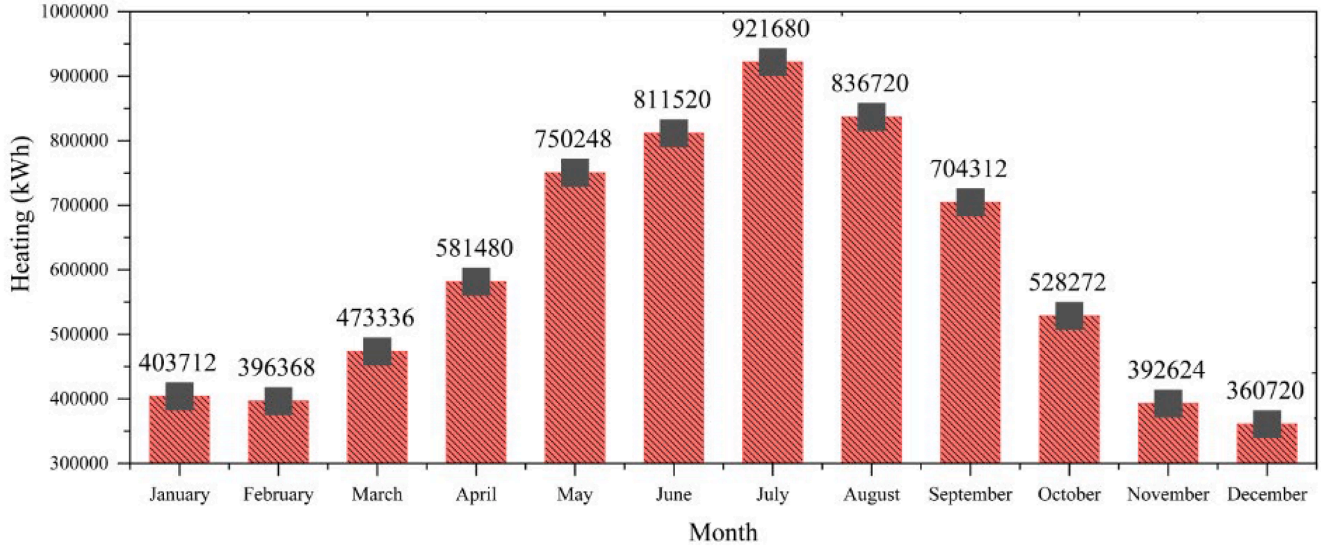

Fig. 24. The amount of monthly heating production.

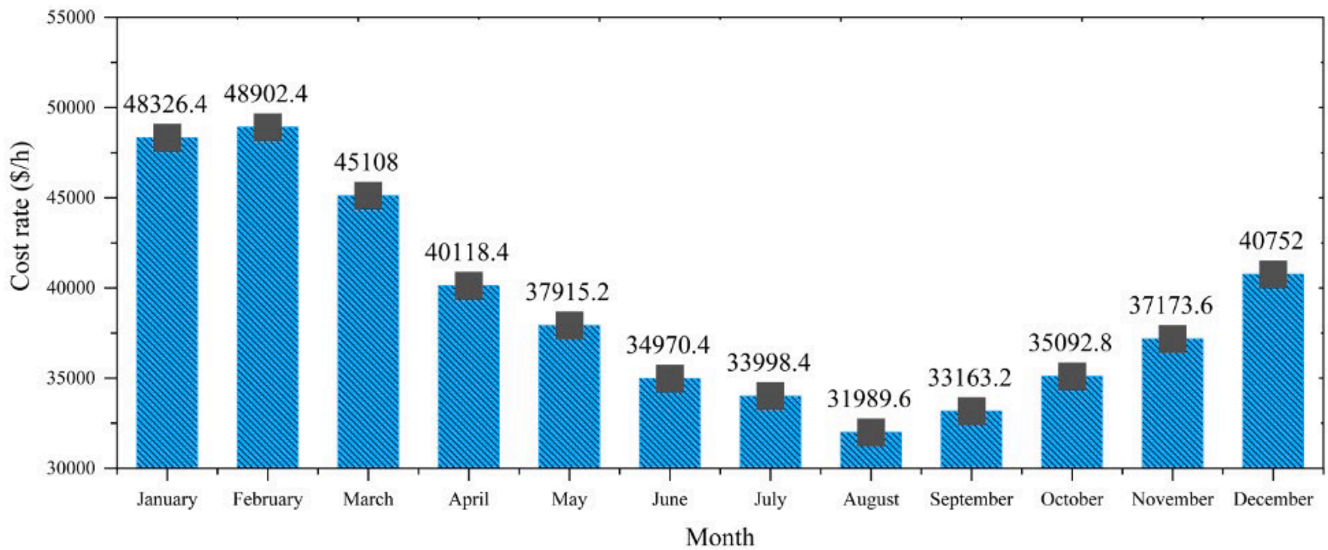

Fig. 25. Monthly cost rate of geothermal power plant.

cooling energy in relation to fluctuations in meteorological parameters. The thermal energy dissipated into the surrounding environment is harnessed for cooling applications, particularly to provide cooling energy to residential buildings. The findings suggest that as the ambient temperature and the temperature of the geothermal energy source increase, the performance of the ORC system diminishes, resulting in a concomitant decrease in the system's cooling production rate.

Fig. 24 depicts the monthly fluctuations in the production of heating energy in relation to fluctuations in meteorological parameters. The thermal energy output from the heat exchanger is harnessed to provide heating for residential buildings throughout the year. The results indicate an augmentation in the heat output from the heat exchanger to the surrounding environment during the warmer months of the year. This observed increase in heat output during the warmer months can be attributed to several factors. As ambient temperatures rise, the temperature differential between the heat exchanger and the environment decreases, leading to a reduction in heat transfer losses. Additionally, the demand for heating in residential buildings typically diminishes during the warmer months, allowing for a greater proportion of the heat output to be dissipated into the environment rather than being utilized for heating purposes.

Fig. 25 illustrates the monthly fluctuations in the cost rate in relation to variations in weather parameters throughout the year. The cost rate is intrinsically linked to the production capacity of the geothermal power plant; as production capacity increases, the cost rate correspondingly rises due to the necessity for larger equipment and increased maintenance requirements. Conversely, a reduction in production capacity leads to a decrease in the cost rate. This relationship highlights the economic implications of operational efficiency in geothermal power generation. During periods of higher production capacity, the demand for more extensive infrastructure and the associated operational costs can lead to elevated cost rates. Conversely, when production capacity declines, the financial burden associated with equipment and maintenance diminishes, resulting in lower overall costs.

Fig. 26 illustrates the changes in the average hourly exergy efficiency per month in relation to variations in weather parameters. Exergy efficiency exhibits a direct correlation with the production power of the geothermal power plant; as the production power increases, so does the exergy efficiency, and vice versa.

In Table 7, the annual technical and economic performance of the

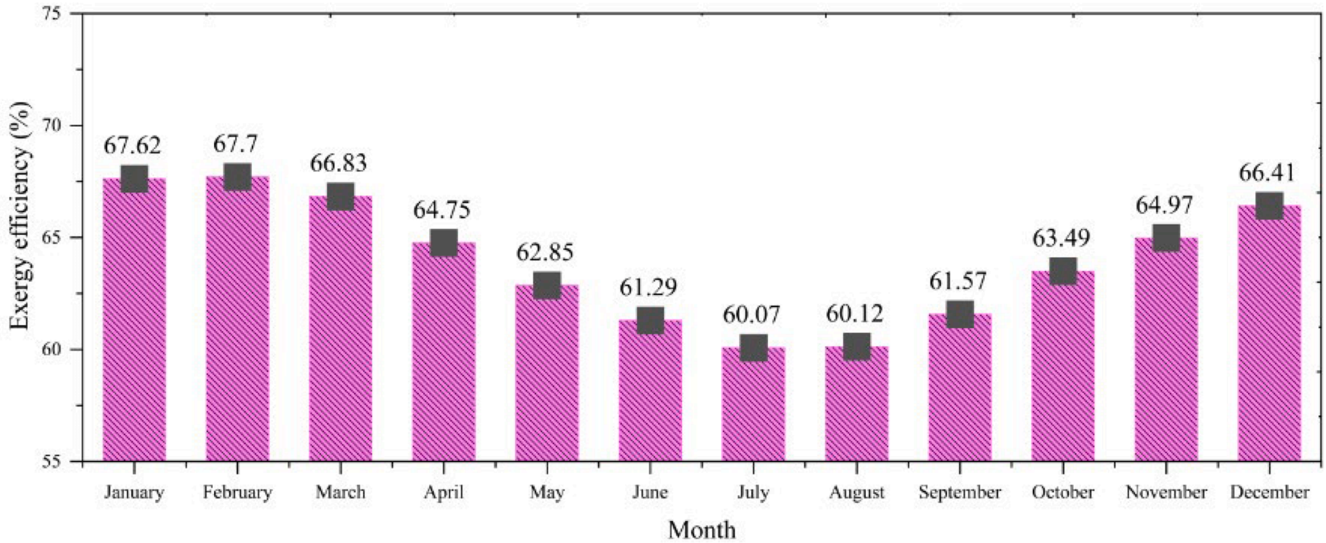

Fig. 26. Monthly exergy efficiency.

Table 7
Annual results of the system on an annual basis.

Output	Value
Output net power (kWh)	2268,324
Cooling (kWh)	2188,196
Heating (kWh)	2091,160
Cost rate ($/h)	467,510.4

system is examined.

4.6. *Environmental analysis*

Copenhagen, Denmark, has been selected as the optimal location for the proposed power plant. Fig. 27 examines the environmental performance of proposed co-generation system.

During the environmental assessment, the following factors were considered:

ü The emission of 0.204 tons of CO2 for each megawatt-hour (MWh) of electricity produced.
ü An environmental cost of $24 associated with the emission of one ton of CO2.
ü An average valuation of $4940 per hectare for non-waterfront bottomland habitat [30–31].

In Table 8, the environmental advantages of the designed system are explained annually for the best study city of Copenhagen.

Table 8
An evaluation of the suggested system's environmental impact.

Net production power (MWh)	Amount of CO_2 emission (ton CO_2/MWh)	Environmental cost ($/ton$CO_2$)	Hectare
10,465.92	2135.048	51,241.14	12

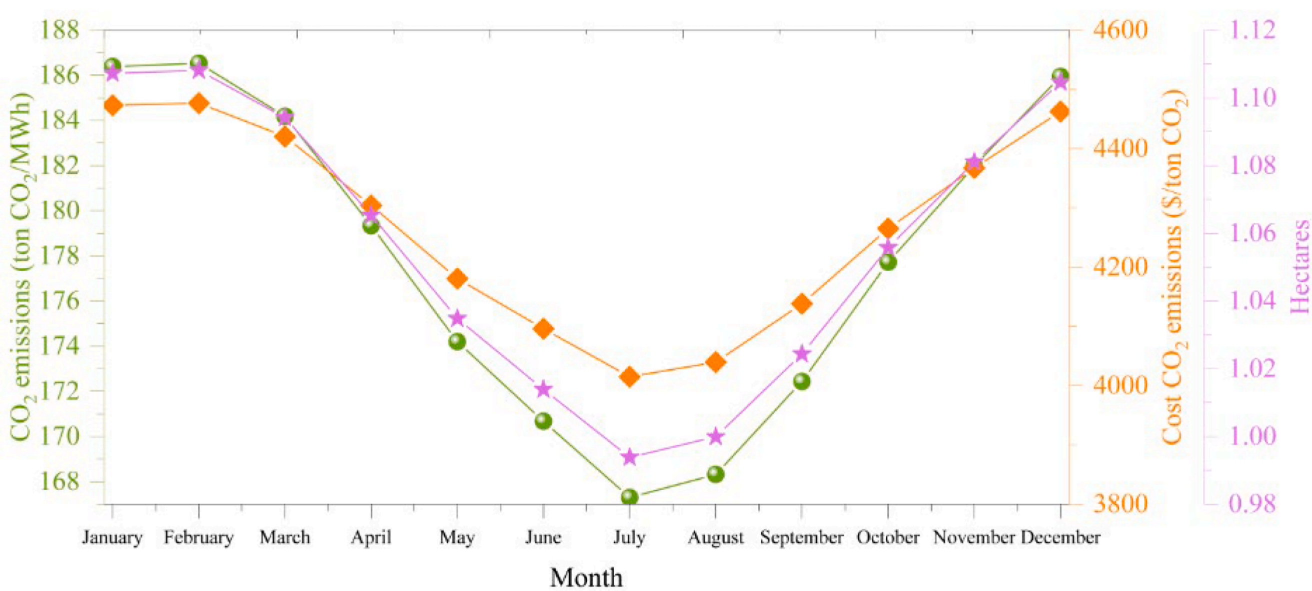

Fig. 27. Environmental performance of the system.

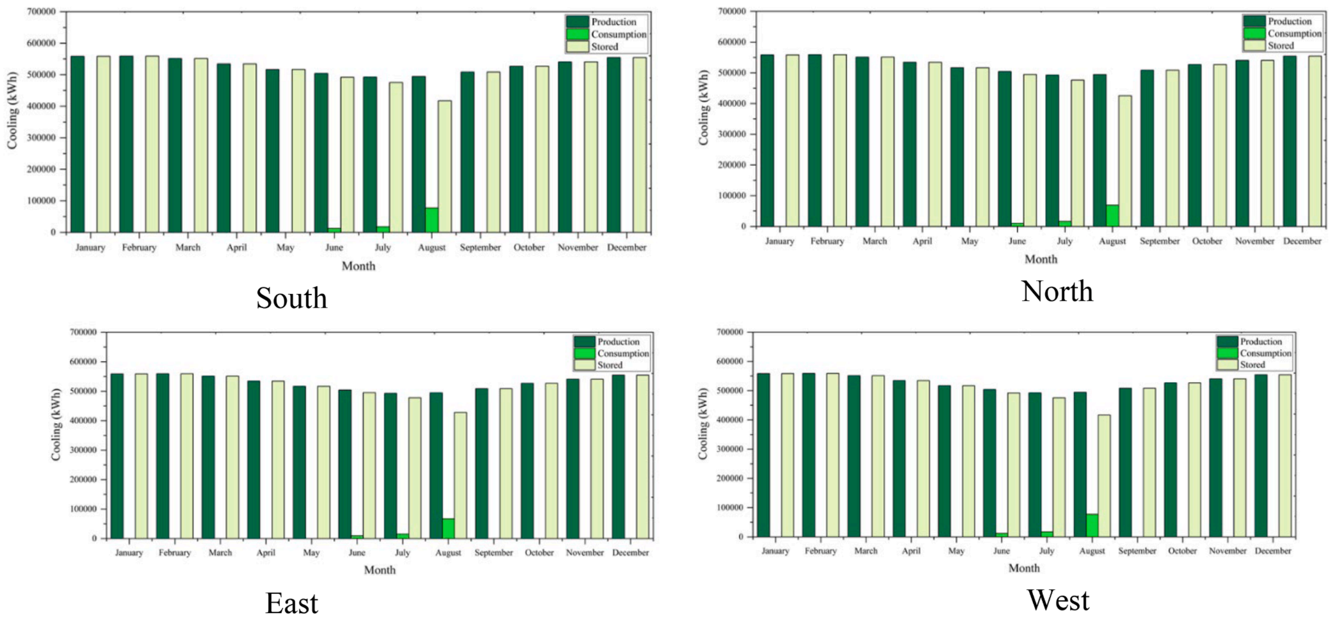

Fig. 28. Stored cooling energy.

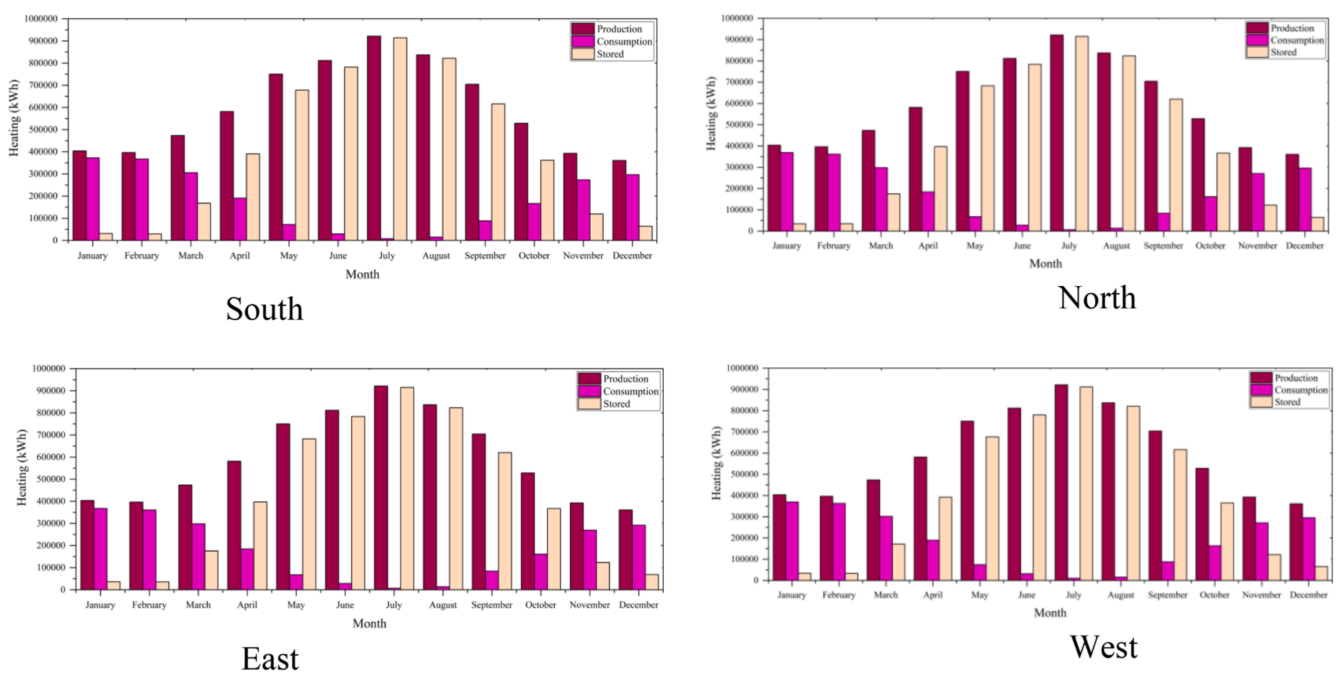

Fig. 29. Stored heating energy.

4.7. Stored energy

The assessment of the system's capacity to meet the energy demands of the building demonstrated its significant capability to provide energy. The results showed that, in addition to meeting the system's energy needs, it produces a sizable excess of heating, cooling, and electricity all year long. This excess energy can be stored for later use or sold to the country's electrical grid. It is important to note that performance of new proposed geothermal co-generation was evaluated in relation to the building's energy consumption across four different scenarios. Figs. 28, 29, and 30 present a monthly analysis of the stored cooling, stored heating, and stored electricity throughout the year. This computation is based on the discrepancy between the energy that the system generates and the energy that the residential building uses. There are also alternative uses for the excess energy that is produced.

The amounts of electricity, heat, and cooling that were stored for the chosen study city during the year are shown in Table 9. This computation shows the possibility of using excess energy for a number of different uses by taking the difference between the energy generated by the system and the energy used by the building.

The results of the analysis regarding the orientation of the building indicated that the minimal cooling energy consumption occurs in the south direction, amounting to 90,511.449 kWh. Conversely, the lowest heating energy consumption is observed in the east direction, totaling 2133,356.825 kWh.

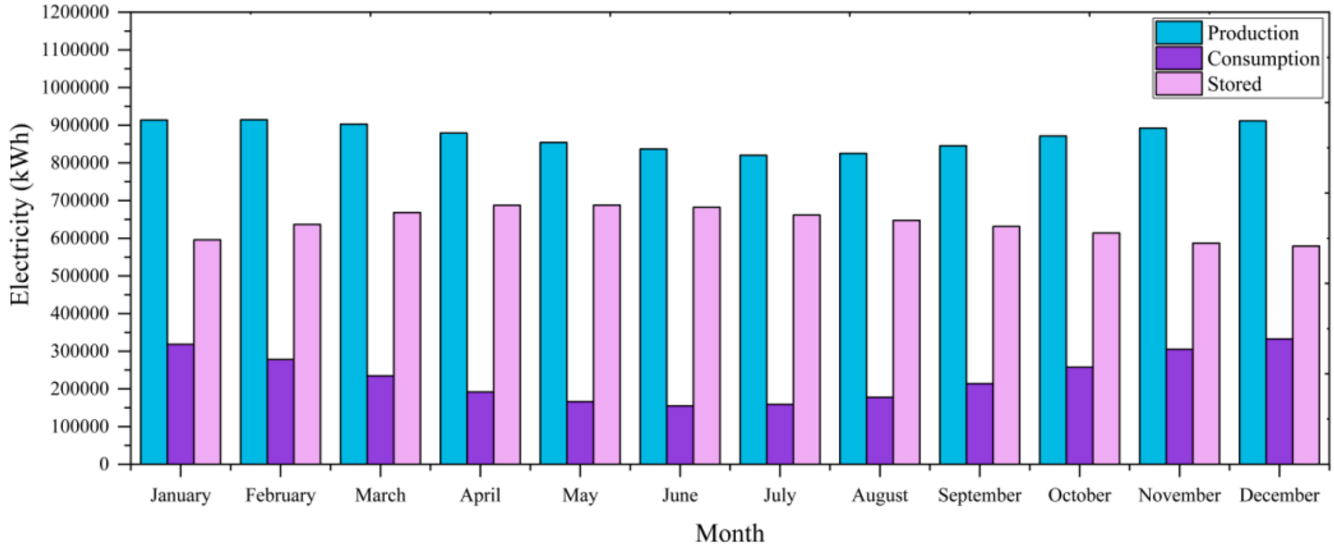

Fig. 30. Stored electrical energy.

Table 9
Stored energy.

Building direction	Energy type	Energy production (kWh)	Energy consumption (kWh)	Stored energy (kWh)
N/S/E/W	Electricity	10,465,920	2789,416	7676,504
North	Cooling	6340,320	106,270.2	6234,050
	Heating	7160,992	2141,172	5019,820
South	Cooling	6340,320	90,511.45	6249,809
	Heating	7160,992	2184,980	4976,012
East	Cooling	6340,320	106,465.7	6233,854
	Heating	7160,992	2133,357	5027,635
West	Cooling	6340,320	94,333.63	6245,986
	Heating	7160,992	2172,425	4988,567

5. Conclusion

This study focuses on the design, optimization of energy consumption, and selection of appropriate materials for constructing a five-story residential building comprising ten units, each with an area of 100 m^2, in Copenhagen, Denmark, with the aim of achieving a zero-energy building definition. The BEopt software was employed to simulate and optimize the energy consumption of the ten-unit residential structure in Copenhagen.

In summary, the innovation and objectives of this research were as follows:

1. Proposing comprehensive changes in energy systems in residential building design: This research aims to introduce general changes in energy systems in the design phase of a residential building, considering its unique energy needs and consumption patterns.
2. Selecting appropriate building materials: Selecting appropriate materials for the construction of residential buildings.
3. Calculating energy consumption: Three main calculations are considered, namely electricity consumption on the one hand and the energy required for heating and cooling. Also, the study building is examined in 4 directions, east, west, north, and south, and the best direction for building construction will be introduced.
4. Optimizing energy consumption and reducing pollution: By implementing energy-saving measures and reducing pollution emissions, the research aims to improve the environmental performance of residential buildings and contribute to sustainable development. Optimization is carried out by software and with a sequential search method.
5. Providing the best hourly energy consumption of the building is carried out to save energy consumption, reduce costs and reducing pollution emissions.
6. Use of renewable energy: This study emphasizes the importance of using renewable energy sources to meet the energy needs of residential buildings, promoting a more sustainable and environmentally friendly approach.
7. Implementation of a renewable multiple generation system: This study proposes a multiple renewable energy generation based on geothermal energy to overcome all its needs throughout the year.
8. Presenting a modified organic Rankine cycle by using an ejector, preheater, and heat recovery vapour generator and simultaneously producing three energies of electricity, cooling, and heating
9. Optimization of system performance and cost reduction: Using the combined optimization methods of neural network and genetic algorithm, this study aims to increase the performance of the solar system and minimize costs, ensuring an economical and efficient energy solution.
10. Providing economic and exergy analyses of the system to introduce the cost and exergy of the components and units of the geothermal system.
11. Environmental Performance Review: This research conducts an environmental performance review of the proposed system, evaluates its environmental impact and sustainability, and provides insights for further improvements.
12. Investigating the system's ability to provide the energy consumed by a residential building and calculating the amount of energy added to the building's consumption.

The findings from the residential building assessment revealed that the annual electricity consumption amounted to 2789,415.522 kWh. To mitigate cooling and heating energy consumption, an analysis was conducted on the building's north, south, east, and west orientations. The results indicated that the lowest cooling energy consumption occurred in the south direction, totaling 90,511.449 kWh, while the east direction recorded the lowest heating energy consumption at 2133,356.825 kWh. A renewable energy system based on geothermal energy was implemented to meet the building's energy requirements, producing three outputs: electricity, cooling, and heating. The proposed geothermal power plant featured a modified ORC integrated with an ejector and a preheater for electricity generation. The waste heat from the ORC evaporator was utilized for cooling, while the output heat from the heat exchanger was employed for heating. Modeling was performed using EES, and the optimization of the proposed system was conducted using AI. The optimization process involved six decision variables: geothermal temperature, geothermal mass flow rate, turbine inlet temperature, evaporator pinch point, pump efficiency, and turbine efficiency, along with two objective functions: η_{ex} and $\dot{C}_{tot}$. The optimal results indicated that the system could achieve an exergy efficiency of 63.79 % and a cost rate of $57.82 per hour. The economic analysis revealed that the HRVG system incurred the highest cost rate among the system components, at $20.06 per hour. A case study was conducted to evaluate the feasibility of implementing new proposed geothermal co-generation system in Denmark, taking into account the impact of Copenhagen's weather data on the power plant's performance. The results demonstrated that the system could generate 10,465,920 kWh of electricity, 6340,320 kWh of cooling, and 7160,992 kWh of heating throughout the year. A comparison of the building's energy consumption and the system's energy production indicated that proposed geothermal co-generation system could adequately meet the energy demands of a five-story, ten-unit residential building in Copenhagen year-round.

The main objective of this research was to investigate the energy consumption of a residential building in different construction directions and in an optimal state, which was designed using simulation software and optimal use of materials and energy. Then, it was followed by the design and use of a multiple production system based on geothermal renewable energy and the production of three products required by buildings, including electricity, cooling, and heating, by a modified organic Rankine cycle to supply building energy based on the potential of the studied area. The proposed system is not only for supplying the energy consumed by buildings but this system can also be used to supply other similar buildings. Because, due to the initial cost of setting up renewable systems and the lack of attention from policymakers and industrialists, the use of a renewable system for a building has not been established in the world and no one supports such systems to supply only one complex in the world. For this reason, it was shown in this research that a small-scale renewable system, in addition to supplying energy to a 5-story residential building in Copenhagen, can produce more surplus energy. Surplus energy can be used to sell to the grid or to other residential, commercial, and industrial buildings and complexes to reduce the costs of the renewable system and cover the initial startup costs. Renewable systems have a high initial cost but have a very low cost over their lifetime and operation. Therefore, by selling the surplus energy of the system, in addition to compensating for the initial costs, compensating for the maintenance and repair costs during operation, one can also think of generating income.

6. Suggestions

To continue this research, future researchers are given suggestions that are reviewed below:

- Investigating environmental parameters and determining the amount of greenhouse gas emissions in the proposed system.
- In the system investigated in the present work, a thermoelectric can be used instead of the condenser in the organic Rankine cycle.
- It is suggested to add the reverse osmosis subsystem to produce fresh water to the system investigated in this work.
- It is suggested to add the multi-effect desalination subsystem, which is used based on thermal energy to produce fresh water, to the system investigated in this work.
- It is possible to use other renewable energy sources as extra energy and to design a combined system to improve the system's efficiency. Among these types of energy, we can mention wind energy, ocean thermal energy, and solar energy.
- Using the storage source in renewable systems for the hours and time when renewable energy is not available, makes the system's efficiency not decrease and the system's stability is maintained in terms of operation.
- Using the battery to store the electricity produced by the system and help during the peak load of residential houses or industries.
- The possibility of using the system in the future in the production of sodium hypochlorite solution used in the purification of drinking water after electrolysis of pure table salt (chloride sodium pure).

CRediT authorship contribution statement

Ehsanolah Assareh: Writing – review & editing, Writing – original draft, Visualization, Validation, Software, Resources, Methodology, Investigation, Formal analysis, Data curation, Conceptualization. **Mohammad Zoghi:** Methodology, Conceptualization. **Ali Zare:** Project administration, Conceptualization. **Hassan Bazazzadeh:** Visualization, Supervision, Software, Resources, Project administration, Methodology, Investigation, Funding acquisition. **Adnan Alboghobeysh:** Formal analysis, Data curation. **Saleh Mobayen:** Investigation, Formal analysis. **Nima Izadyar:** Methodology, Conceptualization. **Siamak Hoseinzadeh:** Project administration, Methodology, Data curation, Conceptualization.

Declaration of competing interest

The authors declare that they have no known competing financial interests or personal relationships that could have appeared to influence the work reported in this paper.

Appendix

Basic relations are utilized in system analysis to verify the thermodynamic analysis of new proposed co-generation system. Appendix 1, Appendix 2

Appendix 1
Basic relations.

relationships	Equation
Law of Survival [Mass]	$\sum_k \dot{m}_i - \sum_k \dot{m}_e = \frac{dm_{cv}}{dt}$
Law of conservation [Energy]	$\dot{Q} - \dot{W} + \sum_i \dot{m}_i\left(h_i + \frac{v_i^2}{2} + gZ_i\right) - \sum_e \dot{m}_e\left(h_e + \frac{v_e^2}{2} + gZ_e\right) = \frac{dE_{cv}}{dt}$
Exergy balance	$\dot{E}x_Q + \sum_i \dot{m}_i(ex_i) = \sum_e \dot{m}_e(ex_e) + \dot{E}x_w + \dot{E}x_D$
Physical exergy	$\dot{E}x_{ph} = \sum_i \dot{m}_i((h_i - h_0) - T_0(s_i - s_0))$

The following assumptions have been established to streamline the analysis:

- Steady state conditions are assumed.
- Both the turbine and pump operate under isentropic conditions.
- Pressure drops in the pipelines are considered negligible [32].
- The output from the condenser is treated as a saturated liquid [32].
- The output from the evaporator is regarded as saturated steam [32].
- Variations in kinetic and potential energy are deemed insignificant [33].

To conduct the thermodynamic analysis of new proposed geothermal system, fundamental relations were employed, which can be further explored in the referenced sources [34–36]. Additionally, to calculate the energy rates, assess the economic performance of each system component, and analyze the proposed system units, relations from pertinent literature were utilized [37–41].

Appendix 2
The amount of input data.

Data	Introduction	Value
T_0	Ambient temperature	25 °C
P_0	Ambient pressure	101.3kpa
T_1	Inlet temperature to Heat recovery vapour generator	210 °C
η_{turbin}	Turbine efficiency	0.85 %
η_{pump}	Pump efficiency	0.9 %
T_4	Inlet temperature to ORC turbine	140 °C
T_{16}	Inlet temperature to ORC ejector	8 °C
$\dot{m}_{GEO}$	Geothermal mass flow rate	10kg/h
pp_{Eva}	Pinch point evaporator	5 °C
pp_{Cond}	Pinch Point Condenser	5 °C

In order to obtain the cost of each part of the system and then the overall cost rate of the system, the cost function of each component is used. The cost rate is obtained using economic parameters such as the capital recovery factor and the interest rate, which allows a better assessment of the cost of the system.

The cost rate of each component is [33–34]:

$$\dot{Z}_k = \frac{Z_k \times CRF \times \varphi}{T} \tag{1}$$

$\dot{Z}_k$ Is the cost rate, φ is the maintenance factor and its value is 1.06. T is the number of system operating hours.

The capital recovery factor is obtained from Eq. (2) [33,34]:

$$CRF = \frac{i(1+i)^n}{(1+i)^n - 1} \tag{2}$$

i and n represent the interest rate and the operating period of the power plant (years), respectively, and are equal to 0.1 and 20, respectively.

To calculate the energy and cost of the system under study in the present study, the relationships in Appendix 3 are used.

Appendix 3
Equations related to energy balance and system cos.

Components	Equation	Equation
Turbine	$Z_{Turbine} = 4750 \times \left(\dot{W}_{turbine}^{0.7}\right) \times \dot{Z}$	$\dot{W}_{tur} = (\dot{m}_4 \times ((h_4 - h_5) + (1 - MMM) * (h_4 - h_5)))$
Pump	$Z_{Pump} = 3540 \times \left(\dot{W}_{Pump}^{0.71}\right) \times \dot{Z}$	$\dot{W}_{pump} = \dot{m}_{13} \times (h_{19} - h_{13})$
Evaporator	$Z_{eva} = 4122 \times \left(A_{eva}^{0.6}\right) \times \dot{Z}$	$Q_{eva} = \dot{m}_{17} \times (h_{17} - h_{18})$
Heat exchanger	$Z_{HEX} = 4122 \times \left(A_{HEX}^{0.6}\right) \times \dot{Z}$	$Q_{HEX} = \dot{m}_2 \times (h_2 - h_3)$
Condenser	$Z_{Cond} = 1773 \times \dot{m}_9 \times \dot{Z}$	$Q_{cond} = \dot{m}_9 \times (h_9 - h_{12})$
Preheater	$Z_{PreH} = 4122 \times \left(A_{PreH}^{0.6}\right) \times \dot{Z}$	$Q_{PreH} = \dot{m}_8 \times (h_8 - h_9)$
Heat recovery vapour generator	$Z_{HRVG} = 4122 \times \left(A_{HRVG}^{0.6}\right) \times \dot{Z}$	$Q_{HRVG} = \dot{m}_1 \times (h_1 - h_2)$
Ejector	$Z_{Ejector} = \left(16.14 \times 989 \times \dot{m}_5 * \left(\left(\frac{T_{16}}{P_{16}}\right)^{0.05}\right) \times P_6^{0.75}\right) \times \dot{Z}$	-
ORC	$Z_{total} = Z_{HRVG} + Z_{PreH} + Z_{Ejector} + Z_{Turbine} + Z_{Cond} + Z_{eva} + Z_{Pump}$	$\dot{W}_{orc} = \dot{W}_{\dot{W}_{tur}} - \dot{W}_{pump}$

The net energy produced by the system is equal to the power produced by the organic Rankine cycle:

$$\dot{W}_{net} = \dot{W}_{ORC} \tag{3}$$

The total cost rate of the system is calculated according to Eq (4):

$$Z_{Total} = Z_{HRVG} + Z_{PreH} + Z_{Ejector} + Z_{HEX} + Z_{Turbine} + Z_{Cond} + Z_{Eva} + Z_{Pump} \tag{4}$$

Efficiency

The exergy efficiency rate of the geothermal system is calculated from Eq (5):

$$\eta_{ex} = \frac{(\dot{W}_{net} + EX_{cooling})}{\dot{E}x_1} \times 100 \quad (5)$$

And the $EX_{cooling}$value is calculated from Eq (6):

$$EX_{cooling} = Q_{eva} \times \left(1 - \frac{T_{18}}{T_0}\right) \quad (6)$$

Exergy efficiency has a direct relationship with the production power of the system, and in other words, exergy efficiency expresses the maximum useful work of the system.

Data availability

No data was used for the research described in the article.

References

[1] G. Axelsson, 7.01 - Introduction to Volume on Geothermal Energy, in: T.M. Letcher (Ed.), Comprehensive Renewable Energy, 2nd Edition, Elsevier, Oxford, 2022, pp. 1–2.
[2] M. Mahmoud, et al., Chapter 2.1 - Introduction and definition of geothermal energy, in: A.G. Olabi (Ed.), Renewable Energy - Volume 2: Wave, Geothermal, and Bioenergy, Academic Press, 2024, pp. 105–120.
[3] T.I. Sigfusson, 01 - Geothermal Energy – Introduction, in: A. Sayigh (Ed.), Comprehensive Renewable Energy, Comprehensive Renewable Energy, 7, Elsevier, Oxford, 2012, pp. 1–2.
[4] T. Uzelli, et al., An Introduction to Geothermal Energy. Reference Module in Earth Systems and Environmental Sciences, Elsevier, 2024.
[5] L. Dingru, et al., Environmental perspectives on the impacts of trade and natural resources on renewable energy utilization in Sub-Sahara Africa: accounting for FDI, income, and urbanization trends, Resour. Policy 80 (2023) 103204.
[6] Y. Jung, et al., A plan to build a net zero energy building in hydrogen and electricity-based energy scenario in South Korea, J. Clean. Prod. 397 (2023) 136537.
[7] R.K. Jaysawal, et al., Concept of net zero energy buildings (NZEB) - A literature review, Clean. Eng. Technol. 11 (2022) 100582.
[8] Z. Mohammadi, et al., Comparative transient assessment and optimization of battery and hydrogen energy storage systems for near-zero energy buildings, Renew. Energy 220 (2024) 119680.
[9] P. Shirazi, et al., Comparison of control strategies for efficient thermal energy storage to decarbonize residential buildings in cold climates: a focus on solar and biomass sources, Renew. Energy 220 (2024) 119681.
[10] M. Mohammadi, et al., Thermo-economic assessment and optimization of a multigeneration system powered by geothermal and solar energy, Appl. Therm. Eng. 230 (2023) 120656.
[11] M.M. Soltani, et al., Techno-economic optimization of a biomass gasification energy system with Supercritical CO2 cycle for hydrogen fuel and electricity production, Fuel 333 (2023) 126264.
[12] M. Alibaba, et al., Thermodynamic, exergo-economic and exergo-environmental analysis of hybrid geothermal-solar power plant based on ORC cycle using emergy concept, Heliyon 6 (4) (2020) e03758.
[13] S. Kavian, C. Aghanajafi, H. Jafari Mosleh, A. Nazari, A. Nazari, Exergy, economic and environmental evaluation of an optimized hybrid photovoltaic-geothermal heat pump system, Appl. Energy 276 (2020).
[14] O.F. Guler, et al., Performance evaluation of a geothermal and solar-based multigeneration system and comparison with alternative case studies: energy, exergy, and exergoeconomic aspects, Renew. Energy 200 (2022) 1517–1532.
[15] W.B. Shumiye, et al., Exergy analysis of solar-geothermal based power plant integrated with boiling, and reverse osmosis water purification, Energy Convers. Manag. X 15 (2022) 100255.
[16] P. Heidarnejad, H. Genceli, M. Asker, S. Khanmohammadi, A comprehensive approach for optimizing a biomass assisted geothermal power plant with freshwater production: techno-economic and environmental evaluation, Energy Convers. Manag. 226 (2020) 113514.
[17] M. Kahraman, A. BahadırOlcay, E. Sorguven, Thermodynamic and thermoeconomic analysis of a 21MW binary type aircooledgeothermal power plant and determination of the effect of ambienttemperature variation on the plant performance, Energy Convers. Manag. 192 (2019) 308–320.
[18] O. Bamisile, et al., Thermo-enviro-exergoeconomic analysis and multi-objective optimization of a novel geothermal-solar-wind micro-multi-energy system for cleaner energy production, Process Safety Environ. Protect. 170 (2023) 157–175.
[19] H. Zhang, et al., Thermodynamic performance analysis of an improved coal-fired power generation system coupled with geothermal energy based on organic Rankine cycle, Renew Energy 201 (2022) 273–290.
[20] B. Tekkanat, et al., The evaluation of hydrogen production via a geothermal-based multigeneration system with 3E analysis and multi-objective optimization, Int. J. Hydrogen Energy 48 (22) (2023) 8002–8021.
[21] M. Haris, et al., A regenerative Enhanced Geothermal System for heat and electricity production as well as energy storage, Renew. Energy 197 (2022) 342–358.
[22] M.H. Khoshgoftar Manesh, et al., Energy, exergy, exergoeconomic, and exergoenvironmental analysis of an innovative solar-geothermal-gas driven polygeneration system for combined power, hydrogen, hot water, and freshwater production, Sustain. Energy Technol. Assess. 51 (2022) 101861.
[23] E. Baniasadi, et al., Exergy-economic analysis of a solar-geothermal combined cooling, heating, power and water generation system for a zero-energy building, Int. J. Hydrogen Energy (2023).
[24] T. Sharmin, et al., A state-of-the-art review on geothermal energy extraction, utilization, and improvement strategies: conventional, hybridized, and enhanced geothermal systems, Int. J. Thermofluids 18 (2023) 100323.
[25] Y. Cao, et al., Development and transient performance analysis of a decentralized grid-connected smart energy system based on hybrid solar-geothermal resources; Techno-economic evaluation, Sustain. Cities Soc. 76 (2022) 103425.
[26] M.S. Alam, et al., An artificial neural network for predicting air traffic demand based on socio-economic parameters, Decis. Anal. J. 10 (2024) 100382.
[27] S. Abut, et al., Paradigm shift from Artificial Neural Networks (ANNs) to deep Convolutional Neural Networks (DCNNs) in the field of medical image processing, Expert Syst. Appl 244 (2024) 122983.
[28] E. Bas, et al., Robust training of median dendritic artificial neural networks for time series forecasting, Expert Syst. Appl. 238 (2024) 122080.
[29] E. Amiri Rad, S. Mohammadi, E. Tayyeban, Simultaneous optimization of working fluid and boiler pressure in an organic Rankine cycle for different heat source temperatures, Energy 194 (2019), https://doi.org/10.1016/j.energy.2019.116856.
[30] (2025). https://www.gov.uk/government/publications/greenhouse-gas-reporting-conversion-factors-.
[31] Kroegera, T., Escobedob, F.J., Hernandezc, J.H., Varelab, S., Delphinb, S., Fishera, J.R.B., Waldrond, J., Reforestation as a novel abatement and compliance measure for ground-level ozone, (2014) 111 (40), https://doi.org/10.1073/pnas.1409785111.
[32] M. Mehrpooya, M. Raeesi, F. Pourfayaz, M. Delpisheh, Investigation of a hybrid solar thermochemical water-splitting hydrogen production cycle and coal-fueled molten carbonate fuel cell power plant, Sustain. Energy Technol. Assess. 47 (2021) 101458.
[33] A.R. Razmi, M. Janbaz, Exergoeconomic assessment with reliability consideration of a green cogeneration system based on compressed air energy storage (CAES), Energy Convers. Manag 204 (October) (2020) 112320. Jan. 2020.
[34] I. Dincer, M.A. Rosen, P. Ahmad. Optimization of Energy Systems, John Wiley & Sons, Ltd, Chichester, UK, 2017.
[35] M. Delpisheh, M.A. Haghghi, H. Athari, M. Mehrpooya, Desalinated water and hydrogen generation from seawater via a desalination unit and a low temperature electrolysis using a novel solar-based setup, Int. J. Hydrogen Energy 46 (2021) 7211–7229.
[36] H. Shakibi, et al., Exergoeconomic and optimization study of a solar and wind-driven plant employing machine learning approaches; a case study of Las Vegas city, J. Clean. Prod. 385 (2023) 135529.
[37] E. Assareh, et al., An integrated system for producing electricity and fresh water from a new gas-fired power plant and a concentrated solar power plant – Case study – (Australia, Spain, South Korea, Iran), Renew. Energy Focus 44 (2023) 19–39.
[38] E. Assareh, M. Delpisheh, E. Farhadi, W. Peng, H. Moghadasi, Optimization of geothermal- and solar-driven clean electricity and hydrogen production multi-generation systems to address the energy nexus, Energy Nexus 5 (2022) 100043.
[39] S.M. Alirahmi, E. Assareh, N. NadakiPourghassab, Green hydrogen & electricity production via geothermal-driven multi-generation system: thermodynamic modeling and optimization, Fuel 308 (2022) 122049.
[40] E. Assareh, M. Assareh, S.M. Alirahmi, M. Shayegh, Thermodynamic assessment of a cogeneration system with CSP Driven-Brayton and Rankine cycles for electric power and hydrogen production in the framework of the energy and water nexus, Energy Nexus (2022) 100031.
[41] S.M. Alirahmi, E. Assareh, Energy, exergy, and exergoeconomics (3E) analysis and multi-objective optimization of a multigeneration energy system for day and night time power generation-Case study: dezful city, Int. J. Hydrogen Energy 45 (56) (2020) 31555–31573.